cells

MDPI

Article

A Preliminary Study on Factors That Drive Patient Variability in Human Subcutaneous Adipose Tissues

Megan K. DeBari [1], Elizabeth K. Johnston [1], Jacqueline V. Scott [1], Erica Ilzuka [1,2], Wenhuan Sun [2], Victoria A. Webster-Wood [1,2] and Rosalyn D. Abbott [1,*]

[1] Department of Biomedical Engineering, Carnegie Mellon University, Pittsburgh, PA 15213, USA; mdebari@andrew.cmu.edu (M.K.D.); elizabej@andrew.cmu.edu (E.K.J.); jacquels@andrew.cmu.edu (J.V.S.); eiizuka@andrew.cmu.edu (E.I.); vwebster@andrew.cmu.edu (V.A.W.-W.)

[2] Department of Mechanical Engineering, Carnegie Mellon University, Pittsburgh, PA 15213, USA; sunwh345@gmail.com

* Correspondence: rabbott@andrew.cmu.edu

Abstract: Adipose tissue is a dynamic regulatory organ that has profound effects on the overall health of patients. Unfortunately, inconsistencies in human adipose tissues are extensive and multifactorial, including large variability in cellular sizes, lipid content, inflammation, extracellular matrix components, mechanics, and cytokines secreted. Given the high human variability, and since much of what is known about adipose tissue is from animal models, we sought to establish correlations and patterns between biological, mechanical, and epidemiological properties of human adipose tissues. To do this, twenty-six independent variables were cataloged for twenty patients, which included patient demographics and factors that drive health, obesity, and fibrosis. A factorial analysis for mixed data (FAMD) was used to analyze patterns in the dataset (with BMI > 25), and a correlation matrix was used to identify interactions between quantitative variables. Vascular endothelial growth factor A (VEGFA) and actin alpha 2, smooth muscle (ACTA2) gene expression were the highest loadings in the first two dimensions of the FAMD. The number of adipocytes was also a key driver of patient-related differences, where a decrease in the density of adipocytes was associated with aging. Aging was also correlated with a decrease in overall lipid percentage of subcutaneous tissue, with lipid deposition being favored extracellularly, an increase in transforming growth factor-β1 (TGFβ1), and an increase in M1 macrophage polarization. An important finding was that self-identified race contributed to variance between patients in this study, where Black patients had significantly lower gene expression levels of TGFβ1 and ACTA2. This finding supports the urgent need to account for patient ancestry in biomedical research to develop better therapeutic strategies for all patients. Another important finding was that TGFβ induced factor homeobox 1 (TGIF1), an understudied signaling molecule, which is highly correlated with leptin signaling, was correlated with metabolic inflammation. Furthermore, this study draws attention to what we define as "extracellular lipid droplets", which were consistently found in collagen-rich regions of the obese adipose tissues evaluated here. Reduced levels of TGIF1 were correlated with higher numbers of extracellular lipid droplets and an inability to suppress fibrotic changes in adipose tissue. Finally, this study indicated that M1 and M2 macrophage markers were correlated with each other and leptin in patients with a BMI > 25. This finding supports growing evidence that macrophage polarization in obesity involves a complex, interconnecting network system rather than a full switch in activation patterns from M2 to M1 with increasing body mass. Overall, this study reinforces key findings in animal studies and identifies important areas for future research, where human and animal studies are divergent. Understanding key drivers of human patient variability is required to unravel the complex metabolic health of unique patients.

Keywords: adipose tissue; patient variability; obesity; inflammation

check for updates

Citation: DeBari, M.K.; Johnston, E.K.; Scott, J.V.; Ilzuka, E.; Sun, W.; Webster-Wood, V.A.; Abbott, R.D. A Preliminary Study on Factors That Drive Patient Variability in Human Subcutaneous Adipose Tissues. *Cells* **2024**, *13*, 1240. https://doi.org/10.3390/cells13151240

Academic Editors: Mirko Manetti, Irene Rosa and Eloisa Romano

Received: 10 June 2024
Revised: 15 July 2024
Accepted: 19 July 2024
Published: 24 July 2024

Copyright: © 2024 by the authors. Licensee MDPI, Basel, Switzerland. This article is an open access article distributed under the terms and conditions of the Creative Commons Attribution (CC BY) license (https://creativecommons.org/licenses/by/4.0/).

1. Introduction

Long thought of as biologically inert, white adipose tissue is now recognized as a highly active endocrine organ that plays a critical role in systemic hormone, cytokine, immune, and metabolic regulation. Given its dynamic state and regulatory role in the body, changes in adipose tissue have profound effects on the health of patients. For example, accumulation of fat mass in obesity is a risk factor for a plethora of diseases from diabetes to certain cancers [1,2]. Furthermore, inconsistencies in human adipose tissues are extensive and multifactorial, including large variability in cellular sizes, lipid content, inflammation, mechanics, extracellular matrix components, and cytokines secreted [3–6]. This large patient variability leads to poor fat graft consistency and survival when the tissue is implanted [7–10] and inadequate treatment options for disorders related to adipose tissue dysfunction. For example, differences in patient demographics such as race and bariatric surgery have led to profound differences in insulin sensitivity between patients [11–16]. Therefore, determining key variables that drive the large variability in human adipose tissue structure and function is critical.

The predominant cell in adipose tissue is the adipocyte, which stores triglycerides that can be released into the blood stream as fatty acids when energy is required. Additional cells make up the stromal vascular fraction (SVF), which is composed of adipose-derived stem cells (ASCs), preadipocytes, immune cells, fibroblasts, pericytes, and endothelial cells [17]. White adipose tissue hosts a variety of resident and infiltrating immune cells, including T and B lymphocytes, macrophages, neutrophils, and eosinophils, that maintain tissue homeostasis [18].

From obese animal models, it is known that adipose tissue acts as a reservoir, buffering nutrient surplus with lipid storage and tissue expansion through adipocyte enlargement (hypertrophy) and formation of new adipocytes (hyperplasia) [19,20]. While adipocyte hypertrophy enables adipose tissue to store more lipids, it decreases the surface area-to-volume ratio, resulting in ineffective nutrient transport and poor cell signaling, promoting tissue dysfunction and metabolic disorders [21]. In fact, hypertrophic adipocyte growth correlates with diabetes in obese humans [12], whereas hyperplastic growth correlates with improved insulin sensitivity in human subjects [22].

To limit adipose tissue expansion, transforming growth factor-β1 (TGFβ1) acts as an inhibitor of adipogenesis [23] and drives fibrotic changes in adipose tissue [24]. Adipose tissue fibrosis is defined as the chronic exposure of adipose tissues to inflammation and hypoxia that leads to a state of extracellular matrix remodeling and collagen deposition [25]. Obesity is one of the main factors leading to fibrosis of adipose tissue [26,27]; however, not every patient that is obese will have fibrotic tissue. Fibrosis is a known contributor to varying patient responses to bariatric surgery [6,28].

Since much of what we know about adipose tissue is from animal models, in this study, we sought to establish correlations and patterns between biological, mechanical, and epidemiological properties of human adipose tissues through statistical analyses (Figure 1). Based on key roles in health, obesity, and fibrosis, 20 independent variables were chosen. The independent variables were paired with six categories of patient demographics (Table 1) that were available for each sample. Here, the ultimate goal was to establish key variables that drive patient variability and to determine if similar findings in human tissues are consistent with those of animal studies. For full demographic information on each patient, see Table 2.

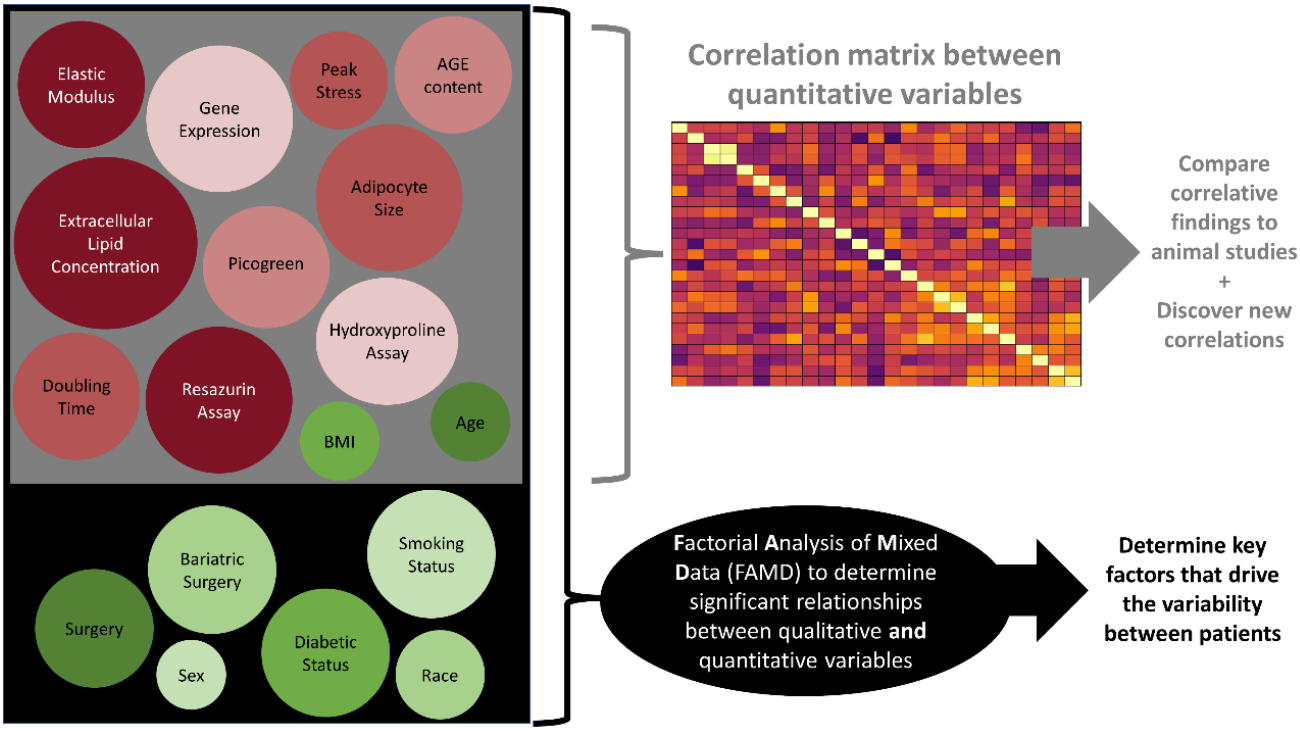


Figure 1. Study design showing how patient demographics (green) and tissue characterization techniques (red) fed into two different statistical models, where (1) each quantitative variable (gray box) was plotted in a correlation matrix against the other quantitative variables to determine correlative relationships and (2) qualitative and quantitative variables (all of the variables in the black box) were fed into a factorial analysis of mixed data (FAMD) to determine significant relationships between the variables. Correlations were used to compare the human data to published data from animal models (i.e., in animals, TGFβ1 gene expression is related to enhanced collagen deposition, and is verified in this study in human samples) and to discover new correlations (i.e., there is a correlation of gene expression between TGIF and leptin). The FAMD indicated what variables account for the most variation in the dataset (with BMI > 25).

Table 1. Breakdown of patient demographics used in this study.

Demographic		Number of Patients
Race	Black	6
	White	14
Sex	Female	17
	Male	3
Surgery	Abdominoplasty	5
	Panniculectomy	15
Bariatric Surgery	Previous Bariatric Surgery	13
	No Bariatric Surgery	7
Diabetic Status	Diabetic	5
	Formerly Diabetic	2
	Not Diabetic	13
Smoking Status	Non-Smoker	11
	Smoker	9

Table 2. Full demographic information for patients used in this study.

Patient	Gender	BMI	Diabetic Status	Smoking Status	Age	Surgery	Weight Loss Method	Race
1	Female	27.06	Formerly Diabetic	Former Smoker	30	Panniculectomy	Gastric Band	White
2	Female	32.12	Not Diabetic	Non-Smoker	68	Panniculectomy	Roux-en-y	White
3	Female	25.92	Not Diabetic	Non-Smoker	54	Abdominoplasty	No Bariatric Surgery	White
4	Female	27.44	Not Diabetic	Former Smoker	49	Panniculectomy	Roux-en-y	White
5	Male	42.26	Diabetic	Former Smoker	51	Panniculectomy	Roux-en-y	White
6	Female	27.4	Not Diabetic	Non-Smoker	50	Panniculectomy	Gastric Band	Black
7	Female	31.6	Not Diabetic	Former Smoker	35	Panniculectomy	Gastric Sleeve	White
8	Female	39.02	Diabetic	Non-Smoker	65	Panniculectomy	Roux-en-y	White
9	Female	43.63	Diabetic	Non-Smoker	38	Panniculectomy	No Bariatric Surgery	Black
10	Male	41.21	Not Diabetic	Non-Smoker	48	Panniculectomy	Roux-en-y	White
11	Female	28.17	Formerly Diabetic	Non-Smoker	35	Abdominoplasty	Roux-en-y	White
12	Female	26.62	Not Diabetic	Former Smoker	43	Panniculectomy	No Bariatric Surgery	Black
13	Female	30.02	Pre-Diabetic	Former Smoker	51	Abdominoplasty	No Bariatric Surgery	White
14	Female	30.05	Not Diabetic	Former Smoker	68	Panniculectomy	Gastric Sleeve	White
15	Female	27.44	Diabetic	Non-Smoker	48	Abdominoplasty	No Bariatric Surgery	White
16	Female	30.23	Diabetic	Non-Smoker	48	Panniculectomy	Roux-en-y	Black
17	Female	31.31	Not Diabetic	Former Smoker	60	Panniculectomy	Gastric Sleeve	White
18	Female	25.34	Not Diabetic	Non-Smoker	38	Abdominoplasty	No Bariatric Surgery	White
19	Female	30.87	Not Diabetic	Smoker	32	Panniculectomy	Gastric Sleeve	Black
20	Male	48.66	Not Diabetic	Non-smoker	44	Panniculectomy	No Bariatric Surgery	Black

2. Methods

2.1. Adipose Tissue Procurement

Discarded, deidentified adipose tissue (n = 20 different patients) was obtained from elective plastic surgery procedures at the University of Pittsburgh Medical Center (UPMC) with the Institutional Review Board (IRB No. 0511186). To randomly select patients, adipose tissue was requested only knowing the surgery type. All patient demographics available were used in analysis of this study, including gender, body mass index (BMI), diabetic status, smoking status, age, surgery the adipose tissue was collected from, previous weight loss strategy, and race (Table 1). Other information, such as comorbidities, was not provided for all patients, so this information was excluded from this study, but it would be advantageous to include in the future. It is important to note that while the patient's diabetic status was provided, the type (type I or type II) was not disclosed. Additionally, because the quantity, duration, and quit date were not provided for patients identified as former smokers, they were grouped with current smokers. This grouping was done to account for residual or long-lasting effects of smoking. Future work should explore this variable further. Adipose tissue was procured from the Adipose Stem Cell Research Center at the University of Pittsburgh's Medical Center's Department of Plastic Surgery. Due to the availability of samples, only overweight and obese patients were obtained (BMI > 25). Subcutaneous adipose tissue samples were dissected from abdominal fat taken from either an abdominoplasty or a panniculectomy surgery. A bulk sample with a minimum size of 4″ by 4″ was used for each experiment. For all testing, samples were taken from directly below the fascia of scarpa.

2.2. Imaging

Tissue samples were isolated from bulk tissue in a 3 × 3 grid. The tissue samples were fixed in formalin (Sigma-Aldrich, St. Louis, MO, USA). Six of the samples were randomly selected and stained with AdipoRed (Lonza, Walkersville, MD, USA) (1:35)

and Alexa Fluor Phalloidin 488 (Thermo Fisher Scientific, Waltham, MA, USA) (1:100) and imaged using confocal and multiphoton microscopy (Nikon, Melville, NY, USA) to visualize lipids, f-actin, and collagen via Second Harmonic Generation. Images taken using confocal microscopy were used to determine the size of extracellular lipid droplets. Two samples per patient were imaged, with two images being captured per sample, for a total of four images per patient and 80 images total for the whole study. A total of 1904 extracellular lipid droplets were measured. Extracellular lipid droplets were defined as lipids that were not intracellularly contained, as indicated by the exclusion from the cytoskeletal Phalloidin staining. The mean diameter was determined to be 7.27 µm, with a standard deviation of 8.16 µm (Figure 2). To encompass a majority of extracellular lipid droplets, the mean plus one standard deviation (15.43 µm) was determined to be the maximum size of what we defined as an extracellular lipid droplet. This accounted for 84.1% of extracellular lipid droplets in the samples imaged and was well below the smallest adipocytes, which are >20 µm [3]. Every patient and field of view had extracellular lipid droplets; however, the number of lipid droplets varied slightly from patient to patient.

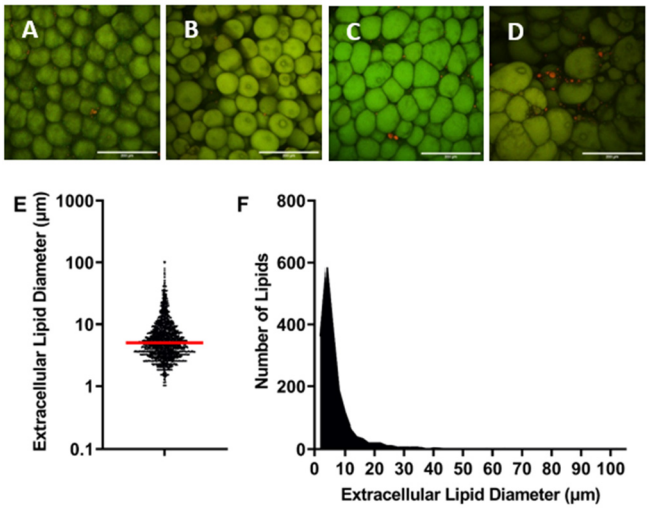


Figure 2. (**A**–**D**) Representative images used to analyze extracellular lipid diameter. Samples were stained with AdipoRed (red) and Phalloidin 488 (green). Extracellular lipids appear red, while adipocytes (stained by both AdipoRed and Phalloidin 488) appear green. Scale bars are 200 µm. Each image is from a different patient. (**E**) Each dot on the graph represents an extracellular lipid droplet diameter measurement, with the mean represented by the red line (mean—7.27 µm, standard deviation—8.16 µm). (**F**) Histogram showing frequency of extracellular lipids with specific diameters, where the majority of extracellular lipids measured were under 15 µm. n = 1904.

The extracellular and intracellular lipid droplets and collagen were visualized with multiphoton microscopy. Depending on the sample and the location of the image, the collagen to adipocyte distribution varied. To account for the high variability of collagen/adipocyte distribution, many images were captured and analyzed. Six samples were imaged, with three images being captured per sample, for a total of 360 images. These images were used to evaluate (1) adipocyte diameter; (2) the extracellular lipid percent; and (3) whether extracellular lipids were in high-density collagen areas (fibrotic regions). Only lipid droplets that could be clearly measured were used for analysis. The number of adipocytes and extracellular lipid droplets were counted and used to determine the extracellular lipid percent, defined as

$$Extracellular\ lipid\ percent = \frac{total_{Extracellular\ lipid\ droplets}}{total_{Extracellular\ lipid\ droplets} + total_{Adipocytes}}$$

where $total_{Extracellular\ lipid\ droplets}$ represents the total number of extracellular lipid droplets in each image, and $total_{Adipocytes}$ represents the total number of adipocytes counted in each image. Additionally, the location of the extracellular lipid droplets was categorized by their proximity to collagen. Extracellular lipid droplets embedded in or touching collagen fibrils were identified as "extracellular lipid droplets in collagen". This was used to determine if extracellular lipid droplets were co-localized within the collagen:

$$Co - localization\ Score = \frac{number\ of\ extracellular\ lipid\ droplets\ in\ collagen}{total\ number\ of\ extracellular\ lipid\ droplets}$$

All image analysis measurements were done using ImageJ v1.53k. An average of 528 adipocytes were measured per patient to obtain diameter metrics. All images were taken using the same magnification. For the full set of quantification results for each patient, see Supplement S1.

2.3. DNA Content

PicoGreen assays (Thermo Fisher Scientific, Waltham, MA, USA) were performed on each patient's tissue samples following the manufacturer's procedure to assess DNA content. The DNA content was normalized to the weight of each tissue sample. n = 5 for each patient. Samples were run in technical duplicates.

2.4. Metabolic Activity/Redox Readout

Resazurin (Thermo Fisher Scientific, Waltham, MA, USA) was diluted to 1 mM with phosphate buffered saline (PBS) (pH 7.4). This was diluted further to 0.05 mM solution using cell culture media (DMEM with 10% FBS and 1% Pen-Strep). An amount of 1 mL of the 0.05 mM resazurin/media solution was placed in a 24-well plate with the tissue samples. The samples were incubated at 37 °C for 2.5 h. Using a microplate reader (SpectraMax i3x), the absorbance at 570/600 nm was measured. Absorbance data were normalized to the average DNA content per gram of tissue for each patient. n = 5 for each patient. Samples were run in technical duplicates.

2.5. Collagen Content

Hydroxyproline assays (Sigma-Aldrich, St. Louis, MO, USA) were performed on each patient's tissue samples following the manufacturer's protocol to assess collagen content. Briefly, approximately 10 mg was homogenized in 100 µL of water (exact tissue weight was recorded before homogenization). A total of 100 µL of 12 M HCL was added and hydrolyzed for 3 h. The supernatant was then transferred to a well plate and allowed to evaporate. Chloramine T/Oxidation Buffer and Diluted DMAB Reagent were then added following the manufacturer's protocol. Collagen content was normalized to the weight of the initial tissue sample. n = 1 for each patient. Samples were run in technical duplicates.

2.6. Advanced Glycation End Products (AGE)

AGE assays (Abcam, Cambridge, MA, USA) were performed on each patient's tissue samples. Tissue samples were flash frozen in liquid nitrogen and stored at −80 °C until use. Tissue samples were then suspended in PBS (pH 7.4) (100 mg of tissue to 1 mL of PBS), homogenized, and stored at −20 °C overnight. The following day, homogenized tissues were subjected to two freeze–thaw cycles. An amount of 1 mL of the solution was then centrifuged at 5000× g at room temperature for 5 min. Samples for this assay were taken from right below the lipid layer of the centrifuged homogenized tissue to avoid the lipid layer. The assay was performed following the manufacturer's procedure. n = 1 for each patient. Samples were run in technical duplicates.

2.7. Compression Testing

Tissue samples were compressed to 90% strain at a rate of 1 mm/min using an electromechanical universal testing system (MTS Criterion, MTS, Eden Prairie, MN, USA). The

elastic modulus was determined by the linear portion of the stress strain curve between 60 and 90% strain. The adipose tissue samples had stress-strain curves similar to elastomers [29]. The stress remained low until around 50–60% strain, when it began to increase drastically. A strain range of 60–90% was used to determine the moduli because this is the region of the curve where the extracellular matrix proteins (ECM) are being compressed. It is thought that prior to the drastic increase in stress, adipocytes are being compressed but not to failure. Once the adipocytes are compressed to failure, the stress increases quickly. This is further supported visually by the lipids or "oil" being seen pooling around the sample as the stress began to increase. Each sample was compressed to 90% strain, and at this point, the peak stress was recorded. n = 10 for each patient.

2.8. Stromal Vascular Fraction (SVF) Doubling Time

The SVF was isolated from subcutaneous adipose tissue as described previously [30]. The cells were isolated by mechanically blending the adipose tissue until the texture resembled lipoaspirate. The tissue was then incubated in a collagenase solution (0.1% collagenase, 1% bovine serum albumin, 98.9% phosphate buffer solution) (Thermo Fisher Scientific, Waltham, MA, USA) in a 1:1 ratio for 1 h at 37 °C. Following the incubation, the solution was centrifuged (5 min at 300× g) to isolate the SVF. The cells were resuspended in media (DMEM with 10% FBS and 1% pen-strep), centrifuged, and seeded into flasks. Once cells reached confluency, cells were trypsinized, and 10,000 cells/well were seeded into a 6-well plate to ensure comparable log-phase growth. Media was changed every 2–3 days. A total of 3 images of each well were taken every other day until confluency was reached. Cells were counted, and the doubling time was calculated using the following equation:

$$DT = (t_2 - t_1)\frac{ln(2)}{ln\left(\frac{q_2}{q_1}\right)}$$

where DT = doubling time, t_2 = second time point, t_1 = first time point, q_2 = number of cells at second time point, and q_1 = number of cells at first time point. n = 5 for each patient. Due to a COVID-19 laboratory shutdown, patients 5 and 6 are missing doubling time data. For the complete set of data for each patient related to mechanical properties, collagen content, AGEs, metabolic activity, and doubling rate, see Supplement S2.

2.9. Reverse Transcription Quantitative Real-Time Polymerase Chain Reaction (RT-qPCR)

Tissue samples were flash frozen in liquid nitrogen and stored at −80 °C until RNA isolation. Total RNA was isolated using the RNeasy Lipid Tissue Mini Kit (QIAGEN, Venlo, Netherlands), and concentration was measured using the NanoDrop 2000c spectrophotometer (Thermo Scientific, Waltham, MA, USA). RNA was processed into cDNA using the iScript cDNA Synthesis Kit (Bio-Rad, Hercules, CA, USA). qPCR reactions were performed with 100 ng of cDNA per reaction. Succinate dehydrogenase complex flavoprotein subunit A (SDHA) (ID: 6389) was used as a reference housekeeping gene [31] and interleukin 6 (IL6) (ID: 3569), tumor necrosis factor α (TNFα) (ID: 7124), TGFβ induced factor homeobox 1 (TGIF1) (ID: 7050), leptin (LEP) (ID: 3952), adiponectin (ADIPOQ) (ID: 9370), transforming growth factor β 1 (TGFβ1) (ID: 7040), actin alpha 2, smooth muscle (ACTA2) (ID: 59), CD163 (ID: 9332), CD86 (ID: 942), and vascular endothelial growth factor A (VEGFA) (ID: 7422) were included as genes of interest. All patient and primer combinations were performed with technical duplicates. The CT value was determined through regression analysis performed by the Bio-Rad CFX96 Real-Time System and C1000 Touch Thermal Cycler (Bio-Rad, Hercules, CA, USA). Since there was no control group, only ΔCT was calculated:

$$\Delta CT = CT_{SDHA} - CT_{Target\ gene}$$

Using this formula, higher CT values of the target gene, which indicate lower gene expression, would have lower ΔCT values. A CT of 45 was assigned for genes that were not detected after 40 cycles. For the full set of patient PCR results, see Supplement S3.

2.10. Statistics

Quantitative variables were evaluated for differences between patients using either a one-way ANOVA or two-way ANOVA followed by a Tukey's post-hoc analysis (GraphPad Prism 9.0.0). A one-way ANOVA was used to determine statistical differences between adipocyte diameters, number of extracellular lipid droplets in collagen/total number of extracellular lipid droplets co-localization, elastic moduli, peak stress, doubling time, and metabolic activity. A two-way ANOVA was used to determine statistical differences between the percentages of pixels (collagen/lipids). Comparisons between ancestry of the cells (self-identified "White" versus "Black") were performed with a *t*-test. *p* values less than 0.05 were determined to be statistically significant. All data are represented as mean +/− standard deviation. A factorial analysis for mixed data (FAMD) was performed on the data using R statistics software. To get all of the variables on the same scale, data were standardized before conducting the analysis by subtracting the mean of the dataset from every value and then dividing by the standard deviation [32,33]. Because complete datasets are required to perform an FAMD, the missMDA package was used to estimate the two missing doubling time data points [34] from a COVID-19 lab closure. The FAMD analysis was performed using the FactoMineR package, with additional graphs being created with the factoextra package. Cos2 values were normalized to the highest value in each dimension to determine significant correlations. Coordinates for quantitative and qualitative data for each dimension are included in Supplement S4. R-code used to generate FAMD results is included in Supplement S5. Using the GraphPad Prism statistical software, all quantitative data were used to generate a correlation matrix using the Pearson correlation coefficient with a confidence interval of 95%.

3. Results and Discussion

Dimensionality reduction is used to identify relationships amongst variables and extract patterns in datasets. To determine if there were relationships between variables in our dataset, we used two different statistical models: (1) a correlation matrix to evaluate relationships between quantitative variables (Figure 3) and (2) a factorial analysis of mixed data (FAMD) to understand the relationships between qualitative (race, sex, surgery type, diabetic status, smoking status) and quantitative variables. An FAMD is similar to principal component analysis (quantitative data only) and multiple correspondence analysis (qualitative data only), but both quantitative and qualitative data can be analyzed [34]. With the FAMD, the number of dimensions needed to account for >80% of the variability in our dataset was determined to be nine (Table 3; for full set of coordinates, see Supplement S4). The largest loading was the variable that contributed the most variance in the given dimension, meaning that variability in these key factors was correlated with variability in the rest of the dataset and is an essential contributor to patient-related differences.

Table 3. Eigenvalues and variance determined through factorial analysis of mixed data (FAMD) analysis.

Dimension	Eigenvalue	Variance (%)	Cumulative Variance (%)	Largest Loading
1	4.89	15.29	15.29	VEGFA
2	4.28	13.38	28.67	ACTA2
3	3.68	11.5	40.17	Number of Adipocytes
4	3.52	11.01	51.18	Race
5	3.05	9.52	60.7	Elastic Moduli
6	2.26	7.08	67.78	Diabetic Status
7	1.89	5.91	73.69	Diabetic Status
8	1.84	5.75	79.44	Smoking Status
9	1.53	4.78	84.22	Advanced Glycation End Products

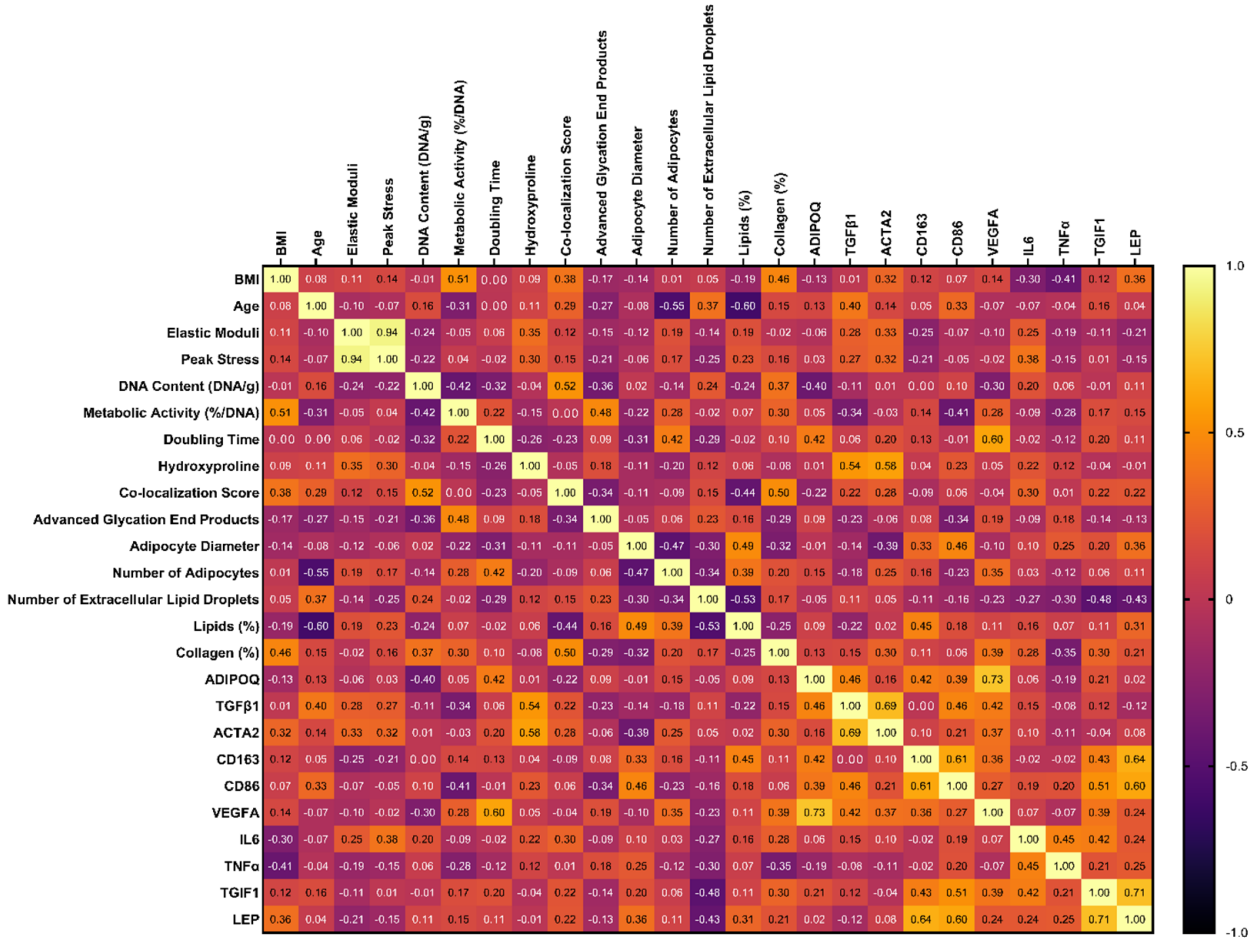


Figure 3. Amongst quantitative variables, many correlations exist in BMI, age, mechanical properties, cell number (DNA content), metabolic activity, doubling time of the stromal vascular fraction, collagen content (hydroxyproline), advanced glycation end products, morphological measurements, histological quantification, and gene expression. The correlation matrix indicates the correlation between quantitative variables (samples from N = 20 patients with BMI > 25). A value greater than 0.7 is considered a high correlation, 0.5–0.7 is considered a moderate correlation, and 0.3–0.5 is considered a low correlation.

3.1. Levels of Vascular Endothelial Growth Factor A (VEGFA) Gene Expression Accounted for the Most Variance in the Full Dataset of Variables (Qualitative and Quantitative)

The variable that contributed the most to the first dimension of the FAMD analysis was gene expression of VEGFA (Table 3). This means that variability in VEGFA gene expression was linked to the most patient-related differences in the other variables in this study. In all individuals, the resident vasculature of adipose tissue acts to ensure adequate blood flow and nutrient/waste transport to allow for adipose tissue expansion and metabolism. In adipose tissue, VEGFA is a pleiotropic molecule that is involved in vasculogenesis, angiogenesis, vascular permeability, tissue remodeling, and metabolic effects (see our recent reviews: [35,36]). Mouse models that overexpress VEGFA result in an increase in adipose tissue vascularization, systemic protection against metabolic dysfunction from a high-fat diet, and higher energy expenditure [37,38]. In the patient population evaluated here, higher gene expression of VEGFA was positively correlated with a longer doubling time of seeded stromal vascular fraction cells (0.60) and higher adiponectin gene expression (0.73) (Figure 4).

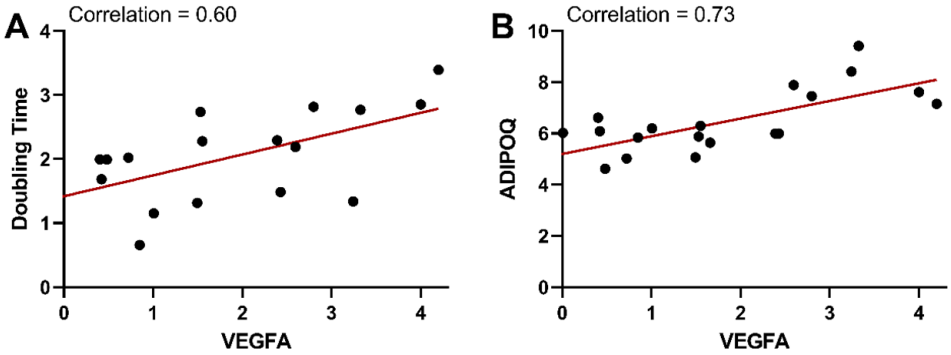


Figure 4. Gene expression of VEGFA was correlated to stromal vascular doubling time and adiponectin gene expression. VEGFA gene expression is plotted versus stromal vascular doubling time (**A**) and adiponectin (ADIPOQ) gene expression (**B**). Gene expression is represented as a delta CT from the housekeeping (HK) gene ($\Delta CT = CT_{SDHA} - CT_{Target\ gene}$). Therefore, the HK gene is equal to 0 on the plots. With the formula used, gene expression is relative to the housekeeping gene and increases at higher values. The red lines indicate a linear regression best fit line for each dataset. Correlations from the correlation matrix are indicated on each plot.

VEGFA is widely expressed in adipose tissue by both the SVF as well as the mature adipocytes [39]. In our study, gene expression was taken from the whole tissue; therefore, the source of the VEGFA signal could be from the vasculature and/or the adipocytes. When the SVF is expanded in vitro, the predominant cells that persist are multilineage ASCs [40]. Therefore, the doubling time in our study reflects the proliferation of the ASCs. Many interacting factors can impact the proliferative capacity of ASCs, for example, diabetes [41], aging [42,43], and certain drugs [44]. However, the correlation between VEGFA and longer ASC doubling time has not been reported. It is well accepted that while proangiogenic, the exogenous application of VEGFA on endothelial cells can have a preferential response to either proliferation or migration depending on the need [45]. One possibility is that similar to endothelial cells, ASCs may have a more migratory response to support angiogenesis. Additionally, in adipose tissue, the balance between stem cell self-renewal and differentiation must be maintained. The regulatory mechanisms for maintaining the stem cell state as well as fate determination are highly conserved. With how heavily intertwined angiogenesis and adipogenesis are, it is not surprising that VEGF is one of these regulators, as blocking VEGFR2, preadipocyte differentiation is also inhibited [46]. Since VEGFA is increased during adipocyte differentiation [46], the positive correlation between VEGFA and a longer doubling time could indicate that the individual is experiencing more hyperplastic adipose tissue growth where ASCs are recruited and differentiate towards adipocytes rather than undergoing proliferation. Supporting this theory, a longer SVF doubling time was also correlated with a higher number of adipocytes (Supplemental Figure S2B, 0.42). Future work should characterize what cells are modulating VEGFA gene expression (the SVF and/or adipocytes) and the relationship between VEGFA and doubling time/adipocyte differentiation. Since endothelial cells represent 10–20% of the SVF [47], future investigations should also evaluate whether the endothelial cell percentage in the SVF affects the overall doubling time of the SVF.

The strong correlation between adiponectin and VEGFA supports findings that adiponectin is down-regulated in VEGFA ablated mice [48,49]. Adiponectin is often considered to be a proangiogenic factor [50,51]. In certain diseases such as chondrosarcoma [52] and rheumatoid arthritis [53], adiponectin promotes VEGFA-dependent angiogenesis. However, other studies have suggested that adiponectin induces endothelial cell apoptosis, reduces their proliferative capacity [54], and inhibits endothelial migration [55]. Therefore, further research is required to discern the correlation observed between adiponectin and VEGFA in the patient population evaluated here. VEGFA is also known to have a protective role in adipose tissue inflammation by recruiting M2 macrophages to adipose depots

in mice [56]. Supporting this finding, our dataset indicated there was a low correlation between VEGFA and CD163 (0.36), with the FAMD indicating that these factors were clustered (Supplement S4). Overall, these findings support a role of adiponectin and M2 macrophage recruitment in VEGFA-mediated metabolic protection.

3.2. TGFβ Induced Factor Homeobox 1 (TGIF1) Gene Expression Was a Key Contributor to the Highest Loading Direction

The second largest contributor in the first dimension of the FAMD was gene expression values for TGIF1 (Figure 5). The role of TGIF1 in adipose tissue has only recently been uncovered. TGIF1 represses TGFβ signaling via multiple pathways, including (1) direct Smad2 inhibition forming a transcriptional repressor complex, (2) prevention of Smad2 phosphorylation, or (3) targeting Smad2 for ubiquitin-dependent degradation [57–59]. In preadipocytes, insulin antagonizes TGFβ signaling in preadipocytes through TGIF1 transcription and is required for the differentiation of preadipocytes [60]. In fact, a recent screening study identified lower TGIF1 transcription as a key reducer of lipid accumulation in differentiating stem cells [61]. TGIF1 positively interacted with leptin, IL6, CD163, CD86, and no bariatric surgery, while negatively interacting with the number of extracellular lipid droplets (Figure 6).

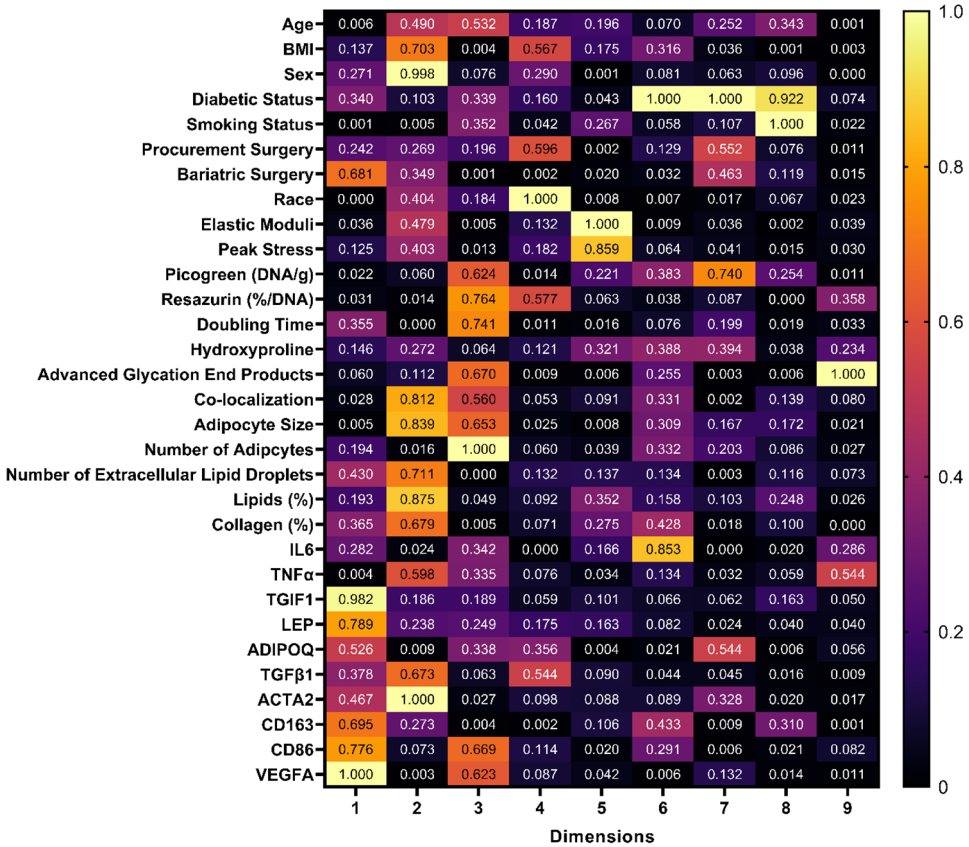


Figure 5. Contribution results generated from the FAMD analysis normalized to the highest contribution in each dimension. In each column, the contribution of variables to the nine dimensions is shown in a heat map, where a value of 1 indicates the largest loading of a variable and the highest contributor in that dimension. For example, in dimension 1, VEGFA is the highest contributor (1.00) followed closely by TGIF1 (0.982).

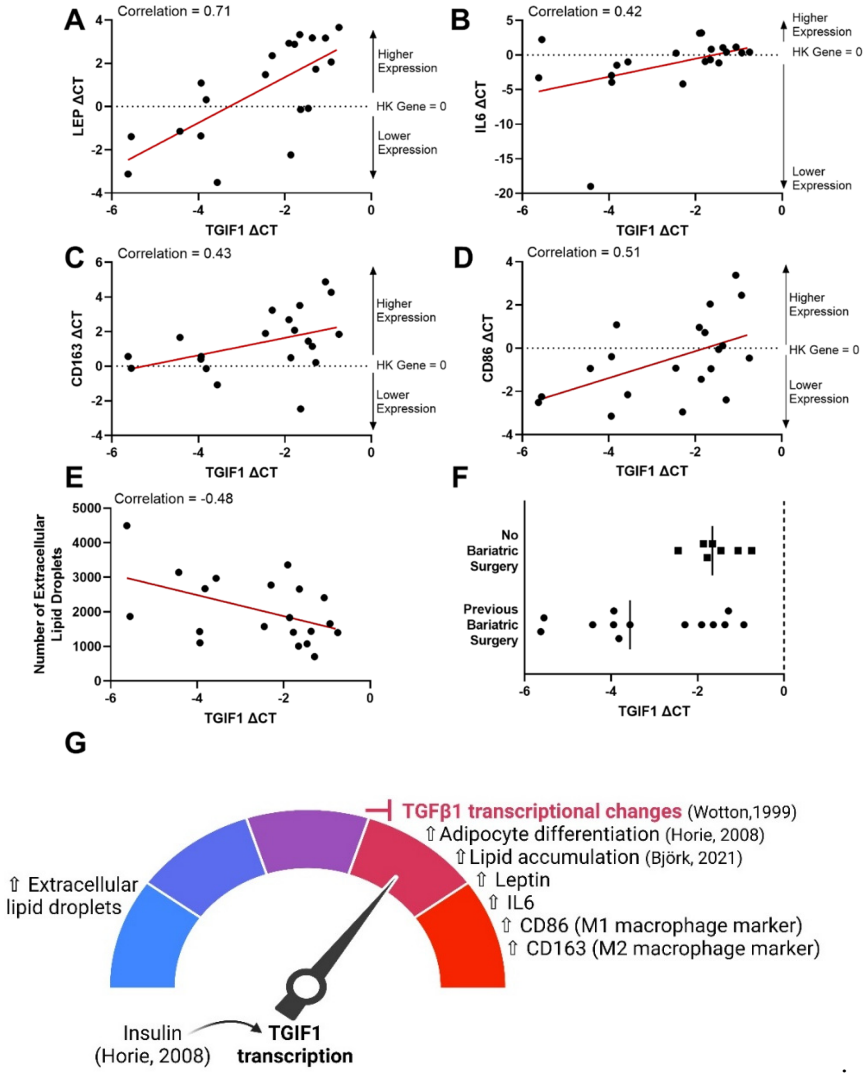


Figure 6. Increased gene expression of transforming growth factor-β induced factor homeobox 1 (TGIF1) was correlated with an increase in gene expression of leptin, interleukin-6 (IL6), CD163, CD86, and no bariatric surgery and a decrease in the number of extracellular lipid droplets. TGIF1 gene expression was plotted versus leptin (LEP) gene expression (**A**), IL6 gene expression (**B**), CD163 gene expression (**C**), CD86 gene expression (**D**), and the number of extracellular lipid droplets counted in histological images (**E**) and separated by whether the patient had undergone bariatric surgery previously or not (**F**). Gene expression is represented as a delta CT from the housekeeping (HK) gene ($\Delta CT = CT_{SDHA} - CT_{Target\ gene}$). Therefore, the HK gene is equal to 0 on the plots. With the formula used, gene expression is relative to the housekeeping gene and increases from a negative value to a higher positive value. The red lines indicate a linear regression best fit line for each dataset. Correlations from the correlation matrix are indicated on each plot. A summary of the results and current literature findings are illustrated (**G**), where the literature indicates that insulin upregulates TGIF1 (Horie, 2008) [60], blocking TGFβ1 transcriptional changes (Wotton, 1999) [57], inducing adipocyte differentiation (Horie, 2008) [60], and increasing lipid accumulation (Bjork, 2021) [61].

Leptin is a pleiotropic hormone predominantly synthesized by adipose tissue that is produced in greater quantities with increasing adipose tissue mass [62]. While leptin is known to stimulate liver fibrosis [63–65], it has been shown to inhibit fibrosis in mouse adipose tissue [66,67]. Our data suggest that TGIF1 could have a role in leptin suppression of fibrosis, as there was a high correlation between higher gene expression levels of TGIF1 and leptin (0.71). It is possible that an increase in leptin stimulates higher TGIF1, suppressing TGFβ-triggered fibrotic changes. However, given the endpoint nature of the study,

causation cannot be determined. Therefore, determining the directionality of the leptin and TGIF1 interaction will be an important next step. Another striking correlation is that lower levels of TGIF1 are correlated with higher numbers of extracellular lipid droplets (−0.48). Further work needs to explore the role of extracellular lipid droplets observed in adipose tissue and their association with TGIF1.

Higher levels of TGIF1 were positively correlated with interleukin-6 (Il6) and macrophage surface markers CD163 and CD86 (Figure 6B–D, respectively), suggesting that high levels of TGIF1 expression could have a role in metabolic inflammation in adipose tissue. Adipocyte secretion of IL6 increases macrophage infiltration in adipose tissue [68] and is linked with reduced insulin sensitivity and diabetes [69]. While both cell surface markers are present on polarized macrophages, CD86 is typically considered to be a classically activated proinflammatory M1 macrophage marker, and CD163 is an alternatively activated anti-inflammatory M2 macrophage marker [70,71]. In the overweight/obese population studied here, CD86 and CD163 were positively correlated (0.61). It is not unusual to see high levels of both CD86 and CD163 gene expression in adipose tissue samples with BMI > 25, as others have noted this signature as indicative of metabolic inflammation [71]. Furthermore, TGIF1 has been identified as a potential transcriptional regulator in macrophage activation [72].

The correlation between TGIF1 gene expression and bariatric surgery is interesting. Bariatric surgery results in rapid weight loss and is an effective treatment to restore insulin sensitivity and reduce type 2 diabetes complications [73,74]. Our results indicated that in some patients, TGIF1 levels of patients who had previously undergone bariatric surgery were well below levels of those who had not (Figure 6F). This is an important finding suggesting that some patients that undergo bariatric surgery will have low levels of TGIF1 and will likely not have TGIF1-mediated TGFβ1 signaling suppression. However, lower levels of TGIF1 were not seen in all patients who underwent surgery, suggesting that other variables also interact.

It is not surprising that TGIF1 and TGFβ1 gene expression levels were not correlated in our adipose tissue samples (0.12). This is because TGIF1 acts downstream from TGFβ1, repressing the transcriptional response [57] rather than affecting the expression of the TGFβ1 gene. This is seen in other tissues as well. For example, in the glomerulus, the profibrotic action of TGFβ1 is antagonized by TGIF and blocks α-smooth muscle activation; however, high levels of TGIF do not affect TGFβ1-mediated Smad2 phosphorylation and its nuclear translocation [75].

3.3. ACTA2 Was the Second Loading Dimension of the FAMD

ACTA2 contributed the most to the second dimension of the FAMD. ACTA2 is a gene that encodes smooth muscle alpha (α)-2 actin production, which is required for cell movement and muscle contraction. ACTA2 (Figure 7) was correlated with TGFβ1 (0.69) and collagen content (0.58), while being inversely related to adipocyte diameter (−0.39). This is consistent with studies where murine adipocytes exposed to a high fat diet upregulate expression of extracellular matrix genes and ACTA2 gene expression characteristic of a myofibroblast-like cell type through reduced PPARγ activity and elevated TGFβ-SMAD signaling [76,77]. The ACTA2 "cellular identity crisis" is thought to drive functionality changes in obese adipose tissues [76], where it is known that enhanced collagen deposition restricts adipocyte size [78]. This was further supported by our dataset's low inverse correlation between collagen percent and adipocyte diameter (−0.32). Collectively, our data suggests a strong role for ACTA2 signaling as a contributor to the variability in human adipose tissues, where high ACTA2 gene expression is related to fibrosis (collagen deposition and TGFβ1) and a reduction in adipocyte cellular diameter.

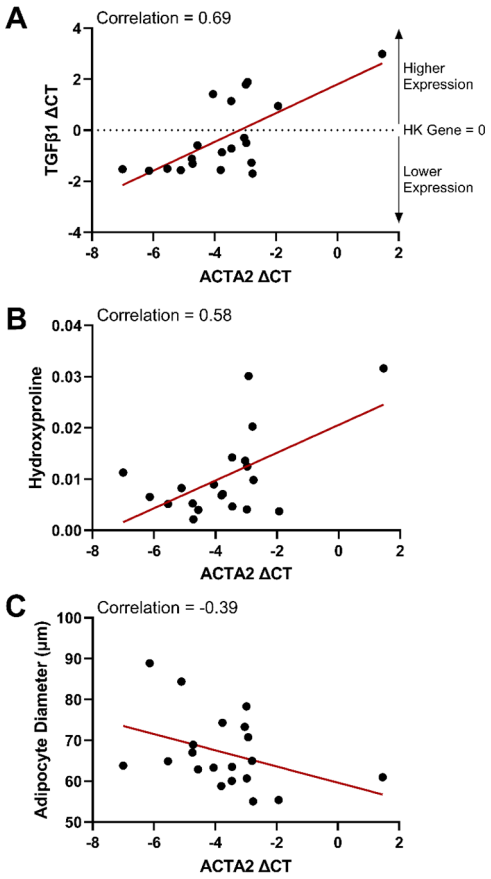


Figure 7. Increased gene expression of actin alpha 2, smooth muscle (ACTA2) gene expression was correlated with an increase in transforming growth factor-β (TGFβ1) gene expression and collagen content (hydroxyproline), with a corresponding decrease in adipocyte diameter. ACTA2 gene expression was plotted versus TGFβ1 (**A**), hydroxyproline content (**B**), and measurements of adipocyte diameter in histological images (**C**). Gene expression is represented as a delta CT from the housekeeping (HK) gene ($\Delta CT = CT_{SDHA} - CT_{Target\ gene}$). Therefore, the HK gene is equal to 0 on the plots. With the formula used, gene expression is relative to the housekeeping gene and increases from a negative value to a higher positive value. The red lines indicate a linear regression best fit line for each dataset. Correlations from the correlation matrix are indicated on each plot.

3.4. TGFβ1 Expression

Besides being correlated with ACTA2 (0.69), as discussed in the last section, TGFβ1 was correlated with hydroxyproline content (0.54), the classically activated M1 macrophage surface marker gene expression (CD86, 0.46), and VEGFA gene expression (0.42). These results are consistent with the known fibrotic role of TGFβ1 in adipose tissue characterized by collagen accumulation, hypoxia (which upregulates VEGFA [79]), and M1 macrophage polarization [25,79–82].

3.5. Age-Related Differences

In our dataset, aging was correlated with a decrease in the number of adipocytes (Figure 8A, −0.549) and percentage of lipids (Figure 8B, −0.601). It is important to note that age and adipocyte size had no correlation (−0.078), indicating that the observed decrease in the number of adipocytes with age was not due to an increase in the size (hypertrophy) of adipocytes. Instead, our findings are consistent with other studies that have shown that hyperplastic growth in adipose tissue declines with age [21]. Furthermore, the decrease in lipid percentage with age and the lack of correlation between BMI and percentage of lipids (−0.186) in our subcutaneous adipose tissue samples support studies that show a shift in lipid storage from subcutaneous to visceral depots with age [62,63]. The ability to buffer

lipids in adipocytes declines with age, leading to ectopic lipid deposition in the liver and muscle [83]. Supporting the shift in adipocyte lipid storage capacity, there was an increase in the number of extracellular lipid droplets with age (Figure 8D, 0.370).

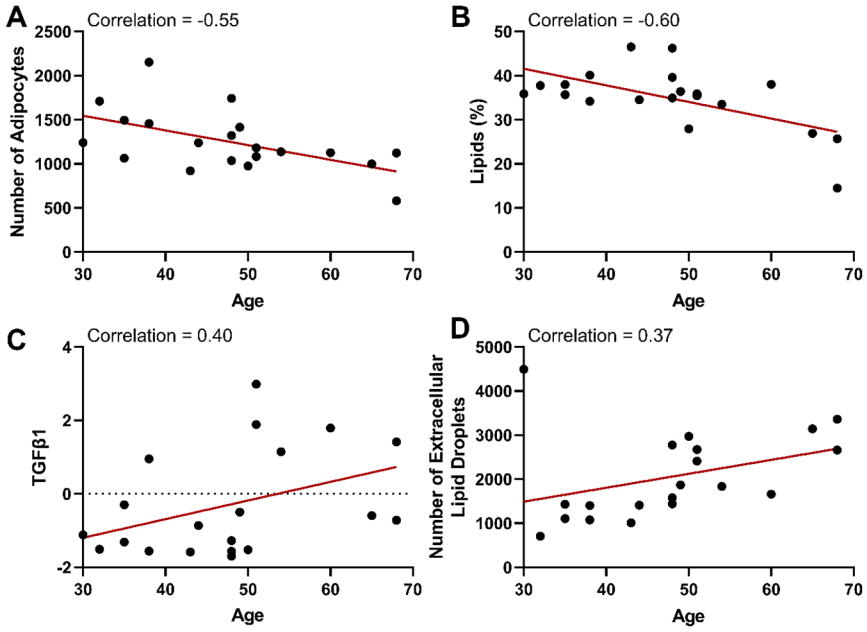


Figure 8. With increasing age, there is a decline in the number of adipocytes and the percentage of lipids and an increase in TGFβ1 and the number of lipid droplets deposited extracellularly. The age of patients at the time of surgery is plotted versus the number of adipocytes measured in histological images (**A**), the lipid percent measured in the same images (**B**), the gene expression of TGFβ1 (**C**), and the number of extracellular lipid droplets counted in histological images (**D**). TGFβ1 gene expression is represented as a delta CT from the housekeeping gene ($\Delta CT = CT_{SDHA} - CT_{Target\ gene}$). With the formula used, gene expression is relative to the housekeeping gene and increases from a negative value to a higher positive value. The red lines indicate a linear regression best fit line for each dataset. Correlations from the correlation matrix are indicated on each plot.

As mentioned previously, aging was correlated with an increase in TGFβ1 gene expression (Figure 8C, 0.40) and upregulation of a M1 macrophage marker (CD86, 0.33) while displaying no correlation with a M2 macrophage marker (CD163, 0.05). It is known that aging results in compounded reactive oxygen species, which readily primes macrophages toward a proinflammatory M1 state and promotes age-related metabolic syndrome (atherosclerosis, obesity, and type II diabetes) [84]. TGFβ signaling largely depends on the cell type and context. However, the upregulation of TGFβ ligands with age is known to contribute to cell degeneration, tissue fibrosis, inflammation, decreased regeneration capacity, and metabolic malfunction in other tissues [85]. Therefore, age-associated changes in subcutaneous adipose tissue are an important context that warrants further investigation.

3.6. Ancestral Differences

Race was the highest loading in the fourth dimension, which accounted for over 11% of the variance in the dataset. Despite known differences in disease prevalence in diverse patient populations, cellular ancestry is largely overlooked in biomedical research [86]. This ancestry-blind approach ignores important differences in disease progression that are key to better therapeutic options, such as ancestral differences in cellular transcription [87] and drug responsiveness [88]. Adipose tissue plays a central role in obesity and type II diabetes progression, with many studies indicating a greater prevalence in Hispanic and Black patients over White patients [89–91].

In the current study, samples derived from self-identified Black patients had significantly lower gene expression levels of TGFβ1 and ACTA2 (Figure 9A,B) and a trend towards lower hydroxyproline collagen content (Figure 9C) than White patients (all patients self-identified as non-Hispanic). As mentioned previously, fibrosis is characterized by enhanced collagen deposition, driven by high levels of TGFβ1 and its target gene ACTA2, which induces a myofibroblastic phenotype [25,77]. TGFβ signals resolution of inflammatory signals, and therefore attenuated TGFβ/Smad signaling results in a reduced mechanism to resolve inflammation [92]. The observed low fibrotic signature in adipose tissues samples derived from Black patients is consistent with Black patients having lower incidences of pulmonary fibrosis than non-Hispanic White patients [93]. Therefore, future work should explore the role of ancestry in subcutaneous adipose tissue fibrosis.

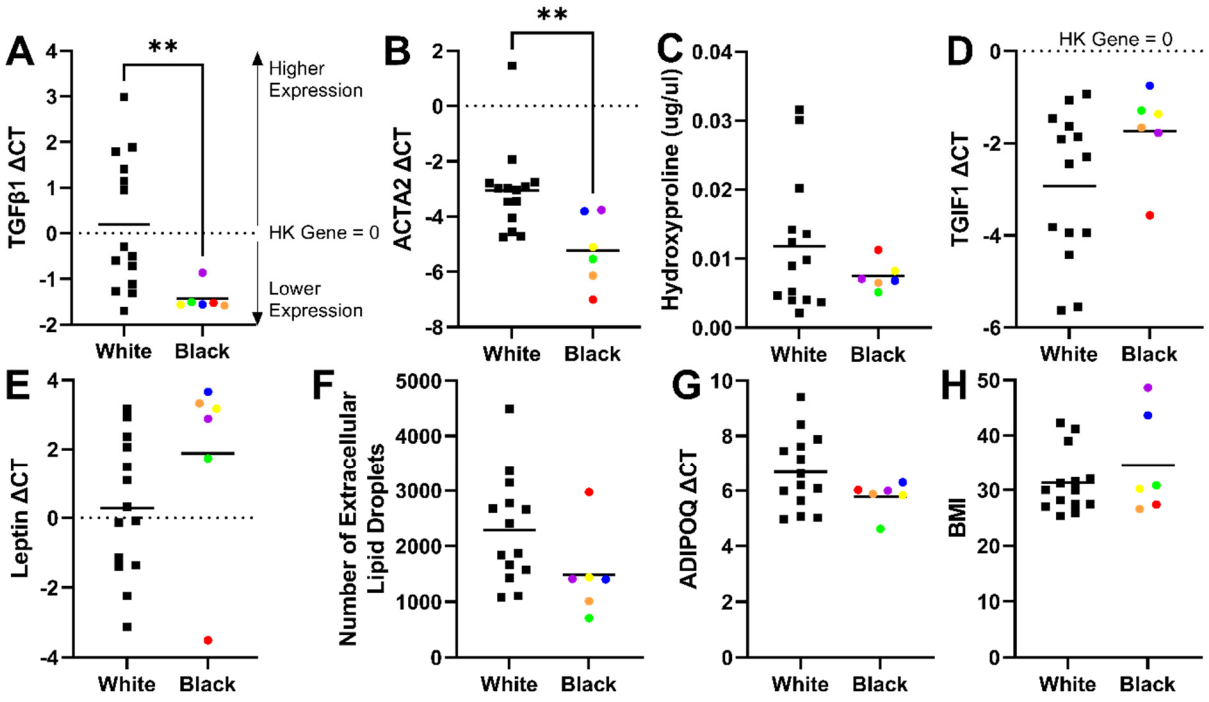


Figure 9. Significantly lower fibrotic gene expression (TGFβ1 and ACTA2) and trends related to collagen content, TGIF1, leptin, extracellular lipid droplets, and adiponectin were observed in self-identified Black patients compared to White patients and were independent of BMI. Samples derived from Black patients had significantly lower gene expression levels of TGFβ1 (**A**) and ACTA2 (**B**) and a trend towards lower hydroxyproline collagen content (**C**) than those derived from White patients (all patients identified as non-Hispanic). On average, samples from Black patients also had higher gene expression levels of TGIF1 (**D**) and leptin (**E**) and fewer extracellular lipid droplets (**F**) compared to White patients. Adiponectin levels were also lower in Black patient samples compared to White patient samples (**G**). Differences between the population groups are independent of body mass index (BMI), as there were no significant differences in BMI between the groups (**H**). Samples derived from Black patients are represented as dots and were color-coded by patient source (i.e., all of the blue dots are from the same patient) to highlight that the outliers in TGIF1, leptin, hydroxyproline, and number of extracellular lipid droplets were all from the same patient (red dots). The patient sample represented by the red dots follows the same trends as the aggregated data (with combined ancestries) where reduced levels of TGIF1 are linked with higher numbers of extracellular lipid droplets and an inability to suppress fibrotic changes in adipose tissue. Samples derived from White patients are represented as black squares. Black lines indicate the mean of the data. Statistical significance was determined by an unpaired *t*-test, where ** indicates $p < 0.01$.

Our data support the concept that disease progression could present differently in different patient populations. For example, there is an observed trend that Hispanic patients

disproportionally develop nonalcoholic fatty liver disease (NAFLD) and have high rates of obesity, visceral adipose tissue, and insulin resistance. In contrast, Black patients tend to have a high prevalence of obesity and insulin resistance with a paradoxically favorable lipid profile and low prevalence of visceral adipose tissue and NAFLD [94]. On average, samples from Black patients in our study had higher gene expression levels of TGIF1 (Figure 9D) and leptin (Figure 9E) with fewer extracellular lipid droplets (Figure 9F) compared to samples from White patients. We speculate that there could be a metabolic phenotype in some patients that favors intracellular lipid accumulation with high TGIF1 transcription that limits extracellular lipid release and (at least initially) favors a diabetic disease process over disease processes that are driven by lipid accumulation in other tissues. This is consistent with a recent study indicating that plasma triglyceride concentrations are lower in African Americans compared to non-Hispanic White, Hispanic White, East Asian, and South Asian ethnicities (controlling for the level of insulin sensitivity) [95]. Furthermore, preliminary findings from another research group indicated that TGIF1 overexpression leads to severe hyperglycemia and obesity-associated diabetes [96], suggesting a link between high TGIF1 signaling and an increased likelihood of developing a diabetic phenotype. The FAMD analysis also identified an interaction between sample ancestry and adiponectin gene expression. While not significant (by an unpaired *t*-test), lower levels of adiponectin were observed in samples derived from Black patients. Adiponectin is an insulin-sensitizing, anti-inflammatory, and anti-diabetic adipokine of which the levels decrease with increasing adipose tissue mass [97–99]. Therefore, lower adiponectin levels (with similar BMI ranges, Figure 9H) further support the higher observed rates of insulin resistance in Black patients compared to White patients [89–91]. Therefore, it is imperative that future work explores TGIF1 signaling, lipid release mechanisms from adipocytes, diabetic disease progression, and mechanisms of inflammation resolution in cells derived from diverse backgrounds.

Interestingly, the outliers in TGIF1, leptin, hydroxyproline, and number of extracellular lipid droplets were all the same patient (red dots). This further supports the aggregated data (with combined ancestries) that indicate that reduced levels of TGIF1 are linked with higher numbers of extracellular lipid droplets and an inability to suppress fibrotic changes in adipose tissue. It should also be noted that our sample size is small for this study, and we had uneven sample sizes for each group, with only six samples from self-identified Black patients and 14 from self-identified White patients. However, even with the small sample size from Black patients, the results are independent of BMI, with a similar spread of BMIs between the groups (Figure 9H). Collectively, these results underscore the urgent need to account for patient ancestry in biomedical research.

3.7. Macrophage Surface Markers

Macrophages play a major role in tissue homeostasis and disease, modulating the growth of tissues as well as tissue remodeling and organization. As mentioned previously, CD86 is considered a classically activated M1 macrophage marker, and CD163 is an alternatively activated M2 macrophage marker [70,71], and both were positively correlated in our dataset (Figure 10A). While macrophage polarization results in distinct functional phenotypes that are often thought of as divergent (i.e., an increase in M1 polarization is associated with a decrease in M2 polarization), induction routes are complex, interconnecting network systems rather than simple switches in activation patterns [100]. While oversimplifying the complexity of macrophage populations, it is well established that lean adipose tissue contains resident macrophages that are alternatively activated (M2) and maintain tissue homeostasis [85]. As adipose tissue increases in mass, there is infiltration of additional macrophages, and the number of classically activated (M1) macrophages increases, contributing to the inflammatory signature of obesity and insulin resistance [101,102], where there is an observed phenotypic switch from one activation state to another [103,104]. However, there is growing evidence that macrophage activation patterns within adipose tissue are more complicated than a full switch from M2 to M1 in obesity where both populations co-exist [105,106], which could be related to significant differences in macrophage

profiles in animals and human models [107]. As mentioned previously, in humans, high levels of both CD86 and CD163 gene expression have been identified in samples from overweight/obese patients [71]. Consistent with this finding, both CD86 and CD163 also showed a high correlation with leptin in our dataset (0.60 and 0.64, respectively), a hormone that is directly related to total body fat mass in humans [41]. Therefore, our results indicate that higher levels of both M1 and M2 polarization markers are present in human subcutaneous adipose tissue with increasing body fat mass. Future work should evaluate the spectrum of polarization states in obese human tissues, including subtype-specific adipose tissue macrophage surface markers [108], to address the complexity of human macrophage populations [109].

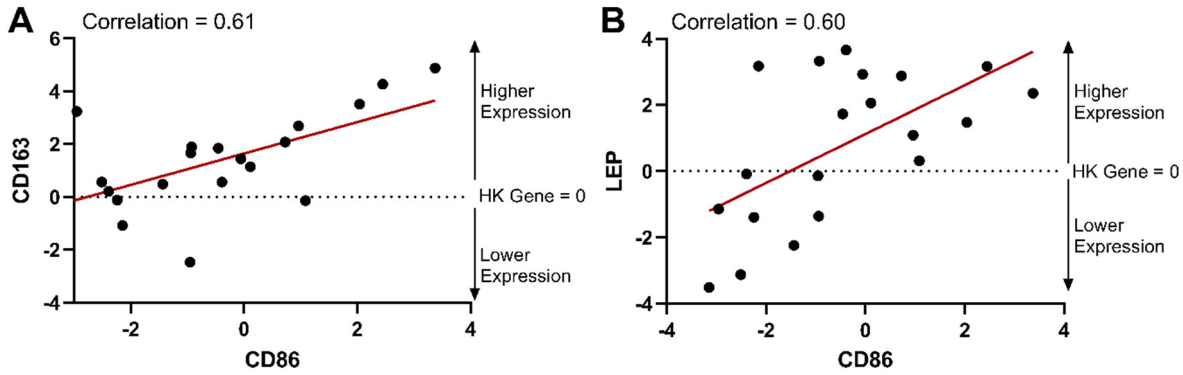


Figure 10. Gene expression of the classically activated CD86 macrophage surface marker and the alternatively activated CD163 surface marker were correlated with each other and with leptin gene expression. CD86 gene expression is plotted versus CD163 gene expression (**A**) and leptin (LEP) gene expression (**B**). Gene expression is represented as a delta CT from the housekeeping (HK) gene ($\Delta CT = CT_{SDHA} - CT_{Target\ gene}$). Therefore, the HK gene is equal to 0 on the plots. With the formula used, gene expression is relative to the housekeeping gene and increases from a negative value to a higher positive value. The red lines indicate a linear regression best fit line for each dataset. Correlations from the correlation matrix are indicated on each plot.

Other correlations that were consistent for both macrophage surface markers, CD86 and CD163, were adipocyte diameter (0.46 and 0.33, respectively) and TGIF1 (mentioned previously and shown in Figure 6). Hypertrophic adipocytes are known to become inflammatory and necrotic, attracting M1 macrophages, which organize into "crown-like" structures that eventually clear necrotic adipocytes [110–112]. M2 macrophages regulate adipose progenitors by initiating proliferation and differentiation into adipocytes to mitigate existing adipocytes' nutritional overload and prevent their further enlargement [113]. Therefore, it is unsurprising that both cell types correlate with hypertrophic adipocytes.

While the macrophage surface markers were correlated in our dataset, there were also distinct correlations associated with each polarization phenotype. For example, higher M1 CD86 gene expression was correlated with TGFβ1 (0.46 versus 0 for CD163), increasing age (0.33 versus 0.05 for CD163), and metabolic activity (−0.41 versus 0.14 for CD163), as discussed previously. Meanwhile, higher M2 CD163 gene expression was correlated with a higher overall lipid percent (0.45 versus 0.18 for CD86), which is likely related to the homeostatic role of M2 macrophages in recruiting the differentiation of new adipocytes [113].

3.8. Diabetic Status and AGEs

The largest loading in dimensions 6 and 7 of the FAMD was diabetic status (Table 3; combined, this accounts for ~12% of the variance). Diabetic status was clustered with AGEs and DNA content for dimensions 6 and 7, respectively (Figure 5). The largest loading in the final dimension of the FAMD (that was included to account for >80% of the variance) was AGEs and was clustered with diabetic status in that dimension as well. The AGE content in the tissue samples varied considerably (Supplemental Figure S3F). However, patients

with diabetes or who formerly had diabetes had higher levels of AGEs. Patients with a higher BMI also had higher levels of AGEs. This trend is supported by literature that shows that increased AGE content in tissue is associated with age, diabetes, and obesity-related complications [114,115].

3.9. Smoking Status

The patients' smoking status was the largest loading in the eighth dimension of the FAMD (Table 3, Figure 5). Adipose tissue has nicotinic receptors [116] that enable tobacco to greatly affect adipose tissue properties and cause downstream effects. The FAMD indicated that diabetic status and smoking were clustered. Diabetic patients who smoke have health problems, comorbidities, and poor outcomes compared to diabetic patients who do not smoke [117–120].

3.10. Limitations

The correlative nature of our investigation limits the conclusions that can be drawn in terms of cause and effect. Instead, we view this study as complementing current literature and informing future research directions into cause-and-effect relationships. It is also important to acknowledge the parameters of this study. The tissue samples used in this study were all from patients who were either overweight or obese (BMI > 25). Therefore, the correlations drawn from the data are not applicable to lean patients. Furthermore, tissue was taken from the subcutaneous adipose depot, and the results are therefore not applicable to other adipose depots in the body. However, it should be noted that there were no significant differences between tissues obtained from abdominoplasty and panniculectomy surgeries. All gene expression values were also taken from the bulk tissue; therefore, cell-type specific gene expression is not possible. For example, an upregulation of ACTA2 could mean that there are more myofibroblasts or that adipocytes are increasing their expression of the gene. As is the case for most studies, this preliminary study of 20 patient samples would be strengthened by the addition of more patients and an increase in the diversity of the patient population. For example, no patient samples were collected from Hispanic backgrounds. Therefore, replicating this study in locations with access to different patient demographics is essential. Assessing the differentiation capacity of ASCs would also have added value to this study and will be considered in future work. Additionally, more information on comorbidities, fat mass (which is more meaningful than BMI), genetics, and other lifestyle information such as history of exercise, diet, and smoking duration and cessation would strengthen and expand these results, providing valuable information for disease treatment and modeling.

4. Conclusions

Many of the results in this study agree with well-established findings in animal studies and other in vitro model systems. For example, TGFβ1 was associated with adipose tissue fibrosis, which is characterized by collagen accumulation and M1 macrophage polarization [25,27,80–82], and diabetes was associated with AGEs [114,115]. This study also revealed new patterns of key markers that drive human variability in adipose tissues.

VEGFA and ACTA2 gene expression were the highest loadings in the first two dimensions of the FAMD, respectively. Vascularization of human adipose tissue varies considerably between patients, and in this study, VEGFA was correlated with adiponectin gene expression. ACTA2 induces a so-called "cellular identity crisis", as described elsewhere [76], which we found was correlated with higher collagen content and TGFβ1 signaling, a reduction in adipocyte cellular diameter, and an upregulation in VEGFA gene expression. There was also a key role of TGIF1 in accounting for variability in the adipose tissues, which has only recently been uncovered. This study emphasizes the importance of TGIF1 signaling for driving patient differences with a strong correlation to leptin signaling.

Furthermore, this study draws attention to what we define as "extracellular lipid droplets", which were consistently found in the obese adipose tissues evaluated here. Re-

duced levels of TGIF1 were correlated with higher numbers of extracellular lipid droplets and an inability to suppress fibrotic changes in adipose tissue. We speculate that there could be a metabolic phenotype in some patients that favors intracellular lipid accumulation with high TGIF1 transcription that limits extracellular lipid release. High values for the colocalization score signify that extracellular lipid droplets were primarily found in collagenous regions of the subcutaneous adipose tissues (consistent across all patients, as seen in Supplemental Figure S1). Further work needs to define what initiates secretion/deposition of lipid droplets extracellularly and whether extracellular lipid droplets have a role and/or association with the progression of adipose tissue fibrosis.

The number of adipocytes was the highest loading in the third dimension of the FAMD, where a decrease in the density of adipocytes was associated with aging and an increase in cellular proliferative capacity of ASCs. Aging was also associated with a decrease in overall lipid percentage that favored extracellular lipid droplet deposition, an increase in TGFβ1, and an increase in M1 macrophage polarization.

The highest loading in the fourth dimension of the FAMD, which accounted for over 11% of the variability in patient-related differences in this study, was self-identified race. While our sample size was small, Black patients had significantly lower gene expression levels of TGFβ1 and ACTA2. This finding indicates there is an urgent need to account for patient ancestry in biomedical research to develop better therapeutic strategies for all patients.

Amongst many other findings, this study indicated that M1 and M2 macrophage markers were correlated with each other and leptin (for BMI > 25). This finding supports growing evidence that macrophage polarization in obesity involves a complex, interconnecting network system rather than a simple switch in activation patterns from M2 to M1 with increasing body mass. Therefore, the characterization of M2 macrophages in overweight/obese tissues warrants further investigation.

Supplementary Materials: The following supporting information can be downloaded at: https://www.mdpi.com/article/10.3390/cells13151240/s1, Supplement S1. Statistical Significance for Image Analysis. Supplemental Figure S1. While there is considerable variability in size of adipocytes, number of adipocytes, and percentage of lipid/collagen, extracellular lipid droplets are consistently found in collagen-dense regions. Supplemental Figure S2. As the number of adipocytes increases the diameter of the remaining adipocytes decreases and the doubling time of the stromal vascular fraction gets longer. Supplemental Table S1. Statistical significance for adipocyte size. Supplemental Table S2. Statistical significance for collagen and lipid pixel percent. Supplement S2. Mechanical properties, DNA content, collagen content, AGEs, metabolic activity, and doubling rate. Supplemental Figure S3. (A) Elastic moduli, (B) Peak Stress, (C) SVF Doubling Time, (D) Metabolic Activity, (E) Hydroxyproline, and (F) Advanced glycation end-product concentration for each patient in the study. Supplemental Figure S4. (A) Elastic moduli, (B) Peak Stress, (C) SVF Doubling Time, (D) Metabolic Activity, (E) Hydroxyproline, and (F) Advanced glycation end-product concentration for each patient in the study. Supplemental Table S3. Statistical significance for elastic modulus. Supplemental Table S4. Statistical significance for peak stress. Supplemental Table S5. Statistical significance for SVF doubling time. Supplemental Table S6. Statistical significance for metabolic activity (resazurin). Supplement S3. Gene Expression. Supplemental Figure S5. Gene expression for each patient shown by the ΔCT value. Supplemental Figure S6. Gene expression of inflammatory cytokines (TNF alpha and interleukin 6) were not correlated with adiponectin, VEGFA, CD86, and CD163. Supplement S4. FAMD coordinates. Supplemental Figure S7. Quantitative variable coordinates in each dimension generated from the FAMD analysis normalized to the furthest coordinate in each dimension. Supplemental Figure S8. Qualitative variable coordinates generated from the FAMD analysis normalized to the furthest coordinate in each dimension. Supplement S5. Code used for running FAMD. References [3,24,25,31,121–135] are cited in the supplementary materials.

Author Contributions: Conceptualization, M.K.D. and R.D.A.; Methodology, M.K.D., E.K.J., J.V.S., W.S., V.A.W.-W. and R.D.A.; Software, M.K.D. and J.V.S.; Validation, M.K.D., E.K.J., J.V.S., W.S. and R.D.A.; Formal analysis, M.K.D. and R.D.A.; Investigation, M.K.D., E.K.J. and E.I.; Resources, V.A.W.-W. and R.D.A.; Data curation, M.K.D., E.K.J. and E.I.; Writing—original draft, M.K.D. and R.D.A.; Writing—review & editing, M.K.D., E.K.J., J.V.S., E.I., W.S., V.A.W.-W. and R.D.A.; Visualization, M.K.D. and R.D.A.; Supervision, V.A.W.-W. and R.D.A.; Project administration, R.D.A.; Funding acquisition, R.D.A. All authors have read and agreed to the published version of the manuscript.

Funding: This work was funded (in part) by the Dowd Fellowship from the College of Engineering at Carnegie Mellon University (M.K.D.). The authors would like to thank Philip and Marsha Dowd for their financial support and encouragement. This work was also funded (in part) through the NIH-T32 Biomechanics and Regenerative Medicine (BiRM) Training Grant (E.K.J.).

Institutional Review Board Statement: The study was conducted in accordance with the Declaration of Helsinki, and approved by the Institutional Review Board at the University of Pittsburgh Medical Center (IRB No. 0511186).

Informed Consent Statement: Not applicable.

Data Availability Statement: The raw data supporting the conclusions of this article will be made available by the authors on request.

Acknowledgments: The authors would like to acknowledge the Department of Plastic Surgery at the University of Pittsburgh's Medical Center and the Adipose Stem Cell Center for procuring tissue samples used in this work. The authors would also like to thank Mallory Griffin for help in isolating tissues and Isabelle Chickanosky and Maya Garg for assisting in gathering doubling time data.

Conflicts of Interest: The authors declare no conflict of interest.

References

1. Wolin, K.Y.; Carson, K.; Colditz, G.A. Obesity and cancer. *Oncologist* **2010**, *15*, 556–565. [CrossRef] [PubMed]
2. Barnes, A.S. The epidemic of obesity and diabetes: Trends and treatments. *Tex. Heart Inst. J.* **2011**, *38*, 142–144. [PubMed]
3. Stenkula, K.G.; Erlanson-Albertsson, C. Adipose cell size: Importance in health and disease. *Am. J. Physiol.-Regul. Integr. Comp. Physiol.* **2018**, *315*, R284–R295. [CrossRef] [PubMed]
4. Abbott, R.D.; Borowsky, F.E.; Alonzo, C.A.; Zieba, A.; Georgakoudi, I.; Kaplan, D.L. Variability in responses observed in human white adipose tissue models. *J. Tissue Eng. Regen. Med.* **2018**, *12*, 840–847. [CrossRef] [PubMed]
5. Alkhouli, N.; Mansfield, J.; Green, E.; Bell, J.; Knight, B.; Liversedge, N.; Tham, J.C.; Welbourn, R.; Shore, A.C.; Kos, K.; et al. The mechanical properties of human adipose tissues and their relationships to the structure and composition of the extracellular matrix. American journal of physiology. *Endocrinol. Metab.* **2013**, *305*, E1427–E1435.
6. Divoux, A.; Tordjman, J.; Lacasa, D.; Veyrie, N.; Hugol, D.; Aissat, A.; Basdevant, A.; Guerre-Millo, M.; Poitou, C.; Zucker, J.-D.; et al. Fibrosis in Human Adipose Tissue: Composition, Distribution, and Link With Lipid Metabolism and Fat Mass Loss. *Diabetes* **2010**, *59*, 2817–2825. [CrossRef] [PubMed]
7. Yi, C.G.; Pan, Y.; Zhen, Y.; Zhang, L.X.; Zhang, X.D.; Shu, M.G.; Han, Y.; Guo, S.Z. Enhancement of viability of fat grafts in nude mice by endothelial progenitor cells. *Dermatol. Surg.* **2006**, *32*, 1437–1443. [PubMed]
8. Rieck, B.; Schlaak, S. Measurement in vivo of the survival rate in autologous adipocyte transplantation. *Plast. Reconstr. Surg.* **2003**, *111*, 2315–2323. [CrossRef] [PubMed]
9. Meier, J.D.; Glasgold, R.A.; Glasgold, M.J. Autologous Fat Grafting Long-term Evidence of Its Efficacy in Midfacial Rejuvenation. *Arch. Facial Plast. Surgey* **2009**, *11*, 24–28. [CrossRef]
10. Report on autologous fat transplantation. ASPRS Ad-Hoc Committee on New Procedures, 30 September 1987. *Plast. Surg. Nurs.* **1987**, *7*, 140–141. [CrossRef]
11. Chabot, K.; Gauthier, M.S.; Garneau, P.Y.; Rabasa-Lhoret, R. Evolution of subcutaneous adipose tissue fibrosis after bariatric surgery. *Diabetes Metab.* **2017**, *43*, 125–133. [CrossRef] [PubMed]
12. Muir, L.A.; Neeley, C.K.; Meyer, K.A.; Baker, N.A.; Brosius, A.M.; Washabaugh, A.R.; Varban, O.A.; Finks, J.F.; Zamarron, B.F.; Flesher, C.G.; et al. Adipose tissue fibrosis, hypertrophy, and hyperplasia: Correlations with diabetes in human obesity. *Obesity* **2016**, *24*, 597–605. [CrossRef] [PubMed]
13. Anand, S.S.; Tarnopolsky, M.A.; Rashid, S.; Schulze, K.M.; Desai, D.; Mente, A.; Rao, S.; Yusuf, S.; Gerstein, H.C.; Sharma, A.M. Adipocyte hypertrophy, fatty liver and metabolic risk factors in South Asians: The Molecular Study of Health and Risk in Ethnic Groups (mol-SHARE). *PLoS ONE* **2011**, *6*, e22112. [CrossRef] [PubMed]
14. Gu, D.; He, J.; Duan, X.; Reynolds, K.; Wu, X.; Chen, J.; Huang, G.; Chen, C.S.; Whelton, P.K. Body weight and mortality among men and women in China. *JAMA* **2006**, *295*, 776–783. [CrossRef] [PubMed]
15. Alba, D.L.; Farooq, J.A.; Lin, M.Y.C.; Schafer, A.L.; Shepherd, J.; Koliwad, S.K. Subcutaneous Fat Fibrosis Links Obesity to Insulin Resistance in Chinese Americans. *J. Clin. Endocrinol. Metab.* **2018**, *103*, 3194–3204. [CrossRef] [PubMed]

16. Jan, V.; Cervera, P.; Maachi, M.; Baudrimont, M.; Kim, M.; Vidal, H.; Girard, P.M.; Levan, P.; Rozenbaum, W.; Lombès, A.; et al. Altered fat differentiation and adipocytokine expression are inter-related and linked to morphological changes and insulin resistance in HIV-1-infected lipodystrophic patients. *Antivir. Ther.* **2004**, *9*, 555–564. [CrossRef] [PubMed]
17. Han, S.; Sun, H.M.; Hwang, K.C.; Kim, S.W. Adipose-Derived Stromal Vascular Fraction Cells: Update on Clinical Utility and Efficacy. *Crit. Rev. Eukaryot. Gene Expr.* **2015**, *25*, 145–152. [CrossRef] [PubMed]
18. Huh, J.Y.; Park, Y.J.; Ham, M.; Kim, J.B. Crosstalk between Adipocytes and Immune Cells in Adipose Tissue Inflammation and Metabolic Dysregulation in Obesity. *Mol. Cells* **2014**, *37*, 365–371. [CrossRef] [PubMed]
19. Verboven, K.; Wouters, K.; Gaens, K.; Hansen, D.; Bijnen, M.; Wetzels, S.; Stehouwer, C.D.; Goossens, G.H.; Schalkwijk, C.G.; Blaak, E.E.; et al. Abdominal subcutaneous and visceral adipocyte size, lipolysis and inflammation relate to insulin resistance in male obese humans. *Sci. Rep.* **2018**, *8*, 4677. [CrossRef]
20. Drolet, R.; Richard, C.; Sniderman, A.D.; Mailloux, J.; Fortier, M.; Huot, C.; Rhéaume, C.; Tchernof, A. Hypertrophy and hyperplasia of abdominal adipose tissues in women. *Int. J. Obes.* **2008**, *32*, 283–291. [CrossRef]
21. Von Bank, H.; Kirsh, C.; Simcox, J. Aging adipose: Depot location dictates age-associated expansion and dysfunction. *Ageing Res. Rev.* **2021**, *67*, 101259. [CrossRef] [PubMed]
22. Arner, E.; Westermark, P.O.; Spalding, K.L.; Britton, T.; Rydén, M.; Frisén, J.; Bernard, S.; Arner, P. Adipocyte turnover: Relevance to human adipose tissue morphology. *Diabetes* **2010**, *59*, 105–109. [CrossRef] [PubMed]
23. Ali, A.T.; Hochfeld, W.E.; Myburgh, R.; Pepper, M.S. Adipocyte and adipogenesis. *Eur. J. Cell Biol.* **2013**, *92*, 229–236. [CrossRef] [PubMed]
24. Khan, T.; Muise, E.S.; Iyengar, P.; Wang, Z.V.; Chandalia, M.; Abate, N.; Zhang, B.B.; Bonaldo, P.; Chua, S.; Scherer, P.E. Metabolic dysregulation and adipose tissue fibrosis: Role of collagen VI. *Mol. Cell. Biol.* **2009**, *29*, 1575–1591. [CrossRef] [PubMed]
25. DeBari, M.K.; Abbott, R.D. Adipose Tissue Fibrosis: Mechanisms, Models, and Importance. *Int. J. Mol. Sci.* **2020**, *21*, 6030. [CrossRef]
26. Shook, B.; Rodeheffer, M.S. Forecasting Fat Fibrosis. *Cell Metab.* **2017**, *25*, 493–494. [CrossRef] [PubMed]
27. Crewe, C.; An, Y.A.; Scherer, P.E. The ominous triad of adipose tissue dysfunction: Inflammation, fibrosis, and impaired angiogenesis. *J. Clin. Investig.* **2017**, *127*, 74–82. [CrossRef] [PubMed]
28. Bel Lassen, P.; Charlotte, F.; Liu, Y.; Bedossa, P.; Le Naour, G.; Tordjman, J.; Poitou, C.; Bouillot, J.L.; Genser, L.; Zucker, J.D.; et al. The FAT Score, a Fibrosis Score of Adipose Tissue: Predicting Weight-Loss Outcome After Gastric Bypass. *J. Clin. Endocrinol. Metab.* **2017**, *102*, 2443–2453. [CrossRef] [PubMed]
29. Comley, K.; Fleck, N. The compressive response of porcine adipose tissue from low to high strain rate. *Int. J. Impact Eng.* **2012**, *46*, 1–10. [CrossRef]
30. Abbott, R.D.; Raja, W.K.; Wang, R.Y.; Stinson, J.A.; Glettig, D.L.; Burke, K.A.; Kaplan, D.L. Long term perfusion system supporting adipogenesis. *Methods* **2015**, *84*, 84–89. [CrossRef]
31. Perez, L.J.; Rios, L.; Trivedi, P.; D'Souza, K.; Cowie, A.; Nzirorera, C.; Webster, D.; Brunt, K.; Legare, J.F.; Hassan, A.; et al. Validation of optimal reference genes for quantitative real time PCR in muscle and adipose tissue for obesity and diabetes research. *Sci. Rep.* **2017**, *7*, 3612. [CrossRef] [PubMed]
32. Carre, A.; Klausner, G.; Edjlali, M.; Lerousseau, M.; Briend-Diop, J.; Sun, R.; Ammari, S.; Reuze, S.; Alvarez Andres, E.; Estienne, T.; et al. Standardization of brain MR images across machines and protocols: Bridging the gap for MRI-based radiomics. *Sci. Rep.* **2020**, *10*, 12340. [CrossRef] [PubMed]
33. Cheadle, C.; Vawter, M.P.; Freed, W.J.; Becker, K.G. Analysis of microarray data using Z score transformation. *J. Mol. Diagn.* **2003**, *5*, 73–81. [CrossRef]
34. Josse, J.; Husson, F. missMDA: A Package for Handling Missing Values in Multivariate Data Analysis. *J. Stat. Softw.* **2016**, *70*, 1–31. [CrossRef]
35. Johnston, E.K.; Abbott, R.D. Adipose Tissue Paracrine-, Autocrine-, and Matrix-Dependent Signaling during the Development and Progression of Obesity. *Cells* **2023**, *12*, 407. [CrossRef] [PubMed]
36. Johnston, E.K.; Abbott, R.D. Adipose Tissue Development Relies on Coordinated Extracellular Matrix Remodeling, Angiogenesis, and Adipogenesis. *Biomedicines* **2022**, *10*, 2227. [CrossRef] [PubMed]
37. Elias, I.; Franckhauser, S.; Bosch, F. New insights into adipose tissue VEGF-A actions in the control of obesity and insulin resistance. *Adipocyte* **2013**, *2*, 109–112. [CrossRef] [PubMed]
38. Sun, K.; Asterholm, I.W.; Kusminski, C.M.; Bueno, A.C.; Wang, Z.V.; Pollard, J.W.; Brekken, R.A.; Scherer, P.E. Dichotomous effects of VEGF-A on adipose tissue dysfunction. *Proc. Natl. Acad. Sci. USA* **2012**, *109*, 5874–5879. [CrossRef]
39. Lemoine, A.Y.; Ledoux, S.; Larger, E. Adipose tissue angiogenesis in obesity. *Thromb. Haemost.* **2013**, *110*, 661–669. [CrossRef]
40. Zuk, P.A.; Zhu, M.; Mizuno, H.; Huang, J.; Futrell, J.W.; Katz, A.J.; Benhaim, P.; Lorenz, H.P.; Hedrick, M.H. Multilineage cells from human adipose tissue: Implications for cell-based therapies. *Tissue Eng.* **2001**, *7*, 211–228. [CrossRef]
41. Moegni, K.; Rosliana, I.; Sobariah, S.; Rosadi, I.; Afini, I.; Widyastuti, T.; Remelia, M.; Sukmawati, D.; Pawitan, J. Diabetes mellitus type 2 reduces the viability, proliferation, and angiogenic marker of adipose-derived stem cells cultured in low-glucose anti-oxidant-serum supplemented medium. *Biomed. Res. Ther.* **2019**, *6*, 3073–3082.
42. Yoshimura, K.; Shigeura, T.; Matsumoto, D.; Sato, T.; Takaki, Y.; Aiba-Kojima, E.; Sato, K.; Inoue, K.; Nagase, T.; Koshima, I. Characterization of freshly isolated and cultured cells derived from the fatty and fluid portions of liposuction aspirates. *J. Cell. Physiol.* **2006**, *208*, 64–76. [CrossRef] [PubMed]

43. Alt, E.U.; Senst, C.; Murthy, S.N.; Slakey, D.P.; Dupin, C.L.; Chaffin, A.E.; Kadowitz, P.J.; Izadpanah, R. Aging alters tissue resident mesenchymal stem cell properties. *Stem Cell Res.* **2012**, *8*, 215–225. [CrossRef]
44. Perez, L.M.; Bernal, A.; de Lucas, B.; San Martin, N.; Mastrangelo, A.; Garcia, A.; Barbas, C.; Galvez, B.G. Altered metabolic and stemness capacity of adipose tissue-derived stem cells from obese mouse and human. *PLoS ONE* **2015**, *10*, e0123397. [CrossRef]
45. Ruhrberg, C.; Gerhardt, H. VEGF and endothelial guidance in angiogenic sprouting. In *VEGF in Development*; Springer: New York, NY, USA, 2008; pp. 68–78.
46. Fukumura, D.; Ushiyama, A.; Duda, D.G.; Xu, L.; Tam, J.; Krishna, V.; Chatterjee, K.; Garkavtsev, I.; Jain, R.K. Paracrine regulation of angiogenesis and adipocyte differentiation during in vivo adipogenesis. *Circ. Res.* **2003**, *93*, E88–E97. [CrossRef]
47. Bourin, P.; Bunnell, B.A.; Casteilla, L.; Dominici, M.; Katz, A.J.; March, K.L.; Redl, H.; Rubin, J.P.; Yoshimura, K.; Gimble, J.M. Stromal cells from the adipose tissue-derived stromal vascular fraction and culture expanded adipose tissue-derived stromal/stem cells: A joint statement of the International Federation for Adipose Therapeutics and Science (IFATS) and the International Society for Cellular Therapy (ISCT). *Cytotherapy* **2013**, *15*, 641–648. [PubMed]
48. Sung, H.-K.; Doh, K.-O.; Son, J.E.; Park, J.G.; Bae, Y.; Choi, S.; Nelson, S.M.L.; Cowling, R.; Nagy, K.; Michael, I.P.; et al. Adipose Vascular Endothelial Growth Factor Regulates Metabolic Homeostasis through Angiogenesis. *Cell Metab.* **2013**, *17*, 61–72. [CrossRef] [PubMed]
49. Gharakhanian, R.; Su, S.; Aprahamian, T. Vascular Endothelial Growth Factor-A Deficiency in Perivascular Adipose Tissue Impairs Macrovascular Function. *Front. Physiol.* **2019**, *10*, 687. [CrossRef]
50. Landskroner-Eiger, S.; Qian, B.; Muise, E.S.; Nawrocki, A.R.; Berger, J.P.; Fine, E.J.; Koba, W.; Deng, Y.; Pollard, J.W.; Scherer, P.E. Proangiogenic contribution of adiponectin toward mammary tumor growth in vivo. *Clin. Cancer Res.* **2009**, *15*, 3265–3276. [CrossRef]
51. Ouchi, N.; Kobayashi, H.; Kihara, S.; Kumada, M.; Sato, K.; Inoue, T.; Funahashi, T.; Walsh, K. Adiponectin Stimulates Angiogenesis by Promoting Cross-talk between AMP-activated Protein Kinase and Akt Signaling in Endothelial Cells. *J. Biol. Chem.* **2004**, *279*, 1304–1309. [CrossRef]
52. Lee, H.P.; Lin, C.Y.; Shih, J.S.; Fong, Y.C.; Wang, S.W.; Li, T.M.; Tang, C.H. Adiponectin promotes VEGF-A-dependent angiogenesis in human chondrosarcoma through PI3K, Akt, mTOR, and HIF-α pathway. *Oncotarget* **2015**, *6*, 36746–36761. [CrossRef]
53. Huang, C.C.; Law, Y.Y.; Liu, S.C.; Hu, S.L.; Lin, J.A.; Chen, C.J.; Wang, S.W.; Tang, C.H. Adiponectin Promotes VEGF Expression in Rheumatoid Arthritis Synovial Fibroblasts and Induces Endothelial Progenitor Cell Angiogenesis by Inhibiting miR-106a-5p. *Cells* **2021**, *10*, 2627. [CrossRef]
54. Bråkenhielm, E.; Veitonmäki, N.; Cao, R.; Kihara, S.; Matsuzawa, Y.; Zhivotovsky, B.; Funahashi, T.; Cao, Y. Adiponectin-induced antiangiogenesis and antitumor activity involve caspase-mediated endothelial cell apoptosis. *Proc. Natl. Acad. Sci. USA* **2004**, *101*, 2476–2481. [CrossRef] [PubMed]
55. Mahadev, K.; Wu, X.; Donnelly, S.; Ouedraogo, R.; Eckhart, A.D.; Goldstein, B.J. Adiponectin inhibits vascular endothelial growth factor-induced migration of human coronary artery endothelial cells. *Cardiovasc. Res.* **2008**, *78*, 376–384. [CrossRef]
56. Elias, I.; Franckhauser, S.; Ferré, T.; Vilà, L.; Tafuro, S.; Muñoz, S.; Roca, C.; Ramos, D.; Pujol, A.; Riu, E. Adipose tissue overexpression of vascular endothelial growth factor protects against diet-induced obesity and insulin resistance. *Diabetes* **2012**, *61*, 1801–1813. [CrossRef]
57. Wotton, D.; Lo, R.S.; Lee, S.; Massagué, J. A Smad transcriptional corepressor. *Cell* **1999**, *97*, 29–39. [CrossRef] [PubMed]
58. Seo, S.R.; Ferrand, N.; Faresse, N.; Prunier, C.; Abécassis, L.; Pessah, M.; Bourgeade, M.-F.; Atfi, A. Nuclear retention of the tumor suppressor cPML by the homeodomain protein TGIF restricts TGF-β signaling. *Mol. Cell* **2006**, *23*, 547–559. [CrossRef] [PubMed]
59. Seo, S.R.; Lallemand, F.; Ferrand, N.; Pessah, M.; L'Hoste, S.; Camonis, J.; Atfi, A. The novel E3 ubiquitin ligase Tiul1 associates with TGIF to target Smad2 for degradation. *EMBO J.* **2004**, *23*, 3780–3792. [CrossRef]
60. Horie, T.; Ono, K.; Kinoshita, M.; Nishi, H.; Nagao, K.; Kawamura, T.; Abe, Y.; Wada, H.; Shimatsu, A.; Kita, T.; et al. TG-interacting factor is required for the differentiation of preadipocytes. *J. Lipid Res.* **2008**, *49*, 1224–1234. [CrossRef]
61. Björk, C.; Subramanian, N.; Liu, J.; Acosta, J.R.; Tavira, B.; Eriksson, A.B.; Arner, P.; Laurencikiene, J. An RNAi screening of clinically relevant transcription factors regulating human adipogenesis and adipocyte metabolism. *Endocrinology* **2021**, *162*, bqab096. [CrossRef]
62. Fried, S.K.; Ricci, M.R.; Russell, C.D.; Laferrère, B. Regulation of Leptin Production in Humans. *J. Nutr.* **2000**, *130*, 3127S–3131S. [CrossRef]
63. Petrescu, A.D.; Grant, S.; Williams, E.; An, S.Y.; Seth, N.; Shell, M.; Amundsen, T.; Tan, C.; Nadeem, Y.; Tjahja, M.; et al. Leptin Enhances Hepatic Fibrosis and Inflammation in a Mouse Model of Cholestasis. *Am. J. Pathol.* **2022**, *192*, 484–502. [CrossRef] [PubMed]
64. Vivoli, E.; Di Maira, G.; Marra, F. Liver Fibrosis and Leptin. *Curr. Pathobiol. Rep.* **2016**, *4*, 69–76. [CrossRef]
65. Saxena, N.K.; Ikeda, K.; Rockey, D.C.; Friedman, S.L.; Anania, F.A. Leptin in hepatic fibrosis: Evidence for increased collagen production in stellate cells and lean littermates of ob/ob mice. *Hepatology* **2002**, *35*, 762–771. [CrossRef] [PubMed]
66. Liu, Y.; Li, Y.; Liang, J.; Sun, Z.; Wu, Q.; Liu, Y.; Sun, C. The Mechanism of Leptin on Inhibiting Fibrosis and Promoting Browning of White Fat by Reducing ITGA5 in Mice. *Int. J. Mol. Sci.* **2021**, *22*, 12353. [CrossRef] [PubMed]
67. Becerril, S.; Rodríguez, A.; Catalán, V.; Mendez-Gimenez, L.; Ramírez, B.; Sainz, N.; Llorente, M.; Unamuno, X.; Gomez-Ambrosi, J.; Frühbeck, G. Targeted disruption of the iNOS gene improves adipose tissue inflammation and fibrosis in leptin-deficient ob/ob mice: Role of tenascin C. *Int. J. Obes.* **2018**, *42*, 1458–1470. [CrossRef]

68. Han, M.S.; White, A.; Perry, R.J.; Camporez, J.-P.; Hidalgo, J.; Shulman, G.I.; Davis, R.J. Regulation of adipose tissue inflammation by interleukin 6. *Proc. Natl. Acad. Sci. USA* **2020**, *117*, 2751–2760. [CrossRef]
69. Rehman, K.; Akash, M.S.H.; Liaqat, A.; Kamal, S.; Qadir, M.I.; Rasul, A. Role of Interleukin-6 in Development of Insulin Resistance and Type 2 Diabetes Mellitus. *Crit. Rev. Eukaryot. Gene Expr.* **2017**, *27*, 229–236. [CrossRef] [PubMed]
70. Jin, X.; Yao, T.; Zhou, Z.E.; Zhu, J.; Zhang, S.; Hu, W.; Shen, C. Advanced glycation end products enhance macrophages polarization into M1 phenotype through activating RAGE/NF-κB pathway. *BioMed Res. Int.* **2015**, *2015*, 732450. [CrossRef]
71. Sindhu, S.; Thomas, R.; Shihab, P.; Al-Shawaf, E.; Hasan, A.; Alghanim, M.; Behbehani, K.; Ahmad, R. Changes in the adipose tissue expression of CD86 costimulatory ligand and CD163 scavenger receptor in obesity and type-2 diabetes: Implication for metabolic disease. *J. Glycom. Lipidom.* **2015**, *5*, 2153-0637. [CrossRef]
72. Ramsey, S.A.; Klemm, S.L.; Zak, D.E.; Kennedy, K.A.; Thorsson, V.; Li, B.; Gilchrist, M.; Gold, E.S.; Johnson, C.D.; Litvak, V.; et al. Uncovering a Macrophage Transcriptional Program by Integrating Evidence from Motif Scanning and Expression Dynamics. *PLoS Comput. Biol.* **2008**, *4*, e1000021. [CrossRef]
73. Maciejewski, M.L.; Arterburn, D.E.; Van Scoyoc, L.; Smith, V.A.; Yancy, W.S., Jr.; Weidenbacher, H.J.; Livingston, E.H.; Olsen, M.K. Bariatric Surgery and Long-term Durability of Weight Loss. *JAMA Surg.* **2016**, *151*, 1046–1055. [CrossRef] [PubMed]
74. Sjöström, L. Review of the key results from the Swedish Obese Subjects (SOS) trial–a prospective controlled intervention study of bariatric surgery. *J. Intern. Med.* **2013**, *273*, 219–234. [CrossRef] [PubMed]
75. Dai, C.; Liu, Y. Hepatocyte growth factor antagonizes the profibrotic action of TGF-beta1 in mesangial cells by stabilizing Smad transcriptional corepressor TGIF. *J. Am. Soc. Nephrol. JASN* **2004**, *15*, 1402–1412. [CrossRef] [PubMed]
76. Roh, H.C.; Kumari, M.; Taleb, S.; Tenen, D.; Jacobs, C.; Lyubetskaya, A.; Tsai, L.T.Y.; Rosen, E.D. Adipocytes fail to maintain cellular identity during obesity due to reduced PPARγ activity and elevated TGFβ-SMAD signaling. *Mol. Metab.* **2020**, *42*, 101086. [CrossRef] [PubMed]
77. Jones, J.E.C.; Rabhi, N.; Orofino, J.; Gamini, R.; Perissi, V.; Vernochet, C.; Farmer, S.R. The Adipocyte Acquires a Fibroblast-Like Transcriptional Signature in Response to a High Fat Diet. *Sci. Rep.* **2020**, *10*, 2380. [CrossRef] [PubMed]
78. Dalmas, E.; Toubal, A.; Alzaid, F.; Blazek, K.; Eames, H.L.; Lebozec, K.; Pini, M.; Hainault, I.; Montastier, E.; Denis, R.G.; et al. Irf5 deficiency in macrophages promotes beneficial adipose tissue expansion and insulin sensitivity during obesity. *Nat. Med.* **2015**, *21*, 610–618. [CrossRef] [PubMed]
79. Anvari, G.; Bellas, E. Hypoxia induces stress fiber formation in adipocytes in the early stage of obesity. *Scientific Reports* **2021**, *11*, 21473. [CrossRef] [PubMed]
80. Reggio, S.; Rouault, C.; Poitou, C.; Bichet, J.-C.; Prifti, E.; Bouillot, J.-L.; Rizkalla, S.; Lacasa, D.; Tordjman, J.; Clément, K. Increased basement membrane components in adipose tissue during obesity: Links with TGFβ and metabolic phenotypes. *J. Clin. Endocrinol. Metab.* **2016**, *101*, 2578–2587. [CrossRef]
81. Liu, L.F.; Kodama, K.; Wei, K.; Tolentino, L.L.; Choi, O.; Engleman, E.G.; Butte, A.J.; McLaughlin, T. The receptor CD44 is associated with systemic insulin resistance and proinflammatory macrophages in human adipose tissue. *Diabetologia* **2015**, *58*, 1579–1586. [CrossRef]
82. Ruggiero, A.D.; Key, C.C.; Kavanagh, K. Adipose Tissue Macrophage Polarization in Healthy and Unhealthy Obesity. *Front. Nutr.* **2021**, *8*, 625331. [CrossRef] [PubMed]
83. Mancuso, P.; Bouchard, B. The Impact of Aging on Adipose Function and Adipokine Synthesis. *Front. Endocrinol.* **2019**, *10*, 137. [CrossRef] [PubMed]
84. Lu, B.; Huang, L.; Cao, J.; Li, L.; Wu, W.; Chen, X.; Ding, C. Adipose tissue macrophages in aging-associated adipose tissue function. *J. Physiol. Sci.* **2021**, *71*, 38. [CrossRef] [PubMed]
85. Tominaga, K.; Suzuki, H.I. TGF-β Signaling in Cellular Senescence and Aging-Related Pathology. *Int. J. Mol. Sci.* **2019**, *20*, 5002. [CrossRef] [PubMed]
86. Moore, E.; Allen, J.B.; Mulligan, C.J.; Wayne, E.C. Ancestry of cells must be considered in bioengineering. *Nat. Rev. Mater.* **2022**, *7*, 2–4. [CrossRef] [PubMed]
87. Bisogno, L.S.; Yang, J.; Bennett, B.D.; Ward, J.M.; Mackey, L.C.; Annab, L.A.; Bushel, P.R.; Singhal, S.; Schurman, S.H.; Byun, J.S. Ancestry-dependent gene expression correlates with reprogramming to pluripotency and multiple dynamic biological processes. *Sci. Adv.* **2020**, *6*, eabc3851. [CrossRef] [PubMed]
88. Ramamoorthy, A.; Pacanowski, M.; Bull, J.; Zhang, L. Racial/ethnic differences in drug disposition and response: Review of recently approved drugs. *Clin. Pharmacol. Ther.* **2015**, *97*, 263–273. [CrossRef] [PubMed]
89. Zhang, Q.; Wang, Y.; Huang, E.S. Changes in racial/ethnic disparities in the prevalence of Type 2 diabetes by obesity level among US adults. *Ethn. Health* **2009**, *14*, 439–457. [CrossRef] [PubMed]
90. Gao, H.X.; Regier, E.E.; Close, K.L. Prevalence of and trends in diabetes among adults in the United States, 1988–2012. *J. Diabetes* **2016**, *8*, 8–9.
91. Hales, C.M.; Carroll, M.D.; Fryar, C.D.; Ogden, C.L. Prevalence of Obesity among Adults and Youth: United States, 2015–2016. 2017. Available online: https://www.cdc.gov/nchs/data/databriefs/db288.pdf (accessed on 18 July 2024).
92. Al-Mulla, F.; Leibovich, S.J.; Francis, I.M.; Bitar, M.S. Impaired TGF-β signaling and a defect in resolution of inflammation contribute to delayed wound healing in a female rat model of type 2 diabetes. *Mol. BioSyst.* **2011**, *7*, 3006–3020. [CrossRef]
93. Swigris, J.J.; Olson, A.L.; Huie, T.J.; Fernandez-Perez, E.R.; Solomon, J.; Sprunger, D.; Brown, K.K. Ethnic and racial differences in the presence of idiopathic pulmonary fibrosis at death. *Respir. Med.* **2012**, *106*, 588–593. [CrossRef]

94. Layden, J.E.; Cotler, S.; Brown, K.A.; Lucey, M.R.; Te, H.S.; Eswaran, S.; Fimmel, C.; Layden, T.J.; Clark, N.M. Racial differences in fibrosis progression after HCV-related liver transplantation. *Transplantation* **2012**, *94*, 178–184. [CrossRef]
95. Raygor, V.; Abbasi, F.; Lazzeroni, L.C.; Kim, S.; Ingelsson, E.; Reaven, G.M.; Knowles, J.W. Impact of race/ethnicity on insulin resistance and hypertriglyceridaemia. *Diabetes Vasc. Dis. Res.* **2019**, *16*, 153–159. [CrossRef] [PubMed]
96. Mo, Y.-Y. Investigating the Role of TGIF in Beta Cell Function and Diabetes; University of Mississippi Medical Center JACKSON United States. 2020. Available online: https://apps.dtic.mil/sti/citations/AD1097373 (accessed on 18 July 2024).
97. Arita, Y.; Kihara, S.; Ouchi, N.; Takahashi, M.; Maeda, K.; Miyagawa, J.I.; Hotta, K.; Shimomura, I.; Nakamura, T.; Miyaoka, K.; et al. Paradoxical decrease of an adipose-specific protein, adiponectin, in obesity. *Biochem. Biophys. Res. Commun.* **1999**, *257*, 79–83. [CrossRef]
98. Hotta, K.; Funahashi, T.; Arita, Y.; Takahashi, M.; Matsuda, M.; Okamoto, Y.; Iwahashi, H.; Kuriyama, H.; Ouchi, N.; Maeda, K. Plasma concentrations of a novel, adipose-specific protein, adiponectin, in type 2 diabetic patients. *Arterioscler. Thromb. Vasc. Biol.* **2000**, *20*, 1595–1599. [CrossRef] [PubMed]
99. Achari, A.E.; Jain, S.K. Adiponectin, a Therapeutic Target for Obesity, Diabetes, and Endothelial Dysfunction. *Int. J. Mol. Sci.* **2017**, *18*, 1321. [CrossRef] [PubMed]
100. Yao, Y.; Xu, X.-H.; Jin, L. Macrophage Polarization in Physiological and Pathological Pregnancy. *Front. Immunol.* **2019**, *10*, 792. [CrossRef] [PubMed]
101. Weisberg, S.P.; McCann, D.; Desai, M.; Rosenbaum, M.; Leibel, R.L.; Ferrante, A.W. Obesity is associated with macrophage accumulation in adipose tissue. *J. Clin. Investig.* **2003**, *112*, 1796–1808. [CrossRef]
102. Xu, H.; Barnes, G.T.; Yang, Q.; Tan, G.; Yang, D.; Chou, C.J.; Sole, J.; Nichols, A.; Ross, J.S.; Tartaglia, L.A. Chronic inflammation in fat plays a crucial role in the development of obesity-related insulin resistance. *J. Clin. Investig.* **2003**, *112*, 1821–1830. [CrossRef]
103. Lumeng, C.N.; Bodzin, J.L.; Saltiel, A.R. Obesity induces a phenotypic switch in adipose tissue macrophage polarization. *J. Clin. Investig.* **2007**, *117*, 175–184. [CrossRef]
104. Lumeng, C.N.; DelProposto, J.B.; Westcott, D.J.; Saltiel, A.R. Phenotypic switching of adipose tissue macrophages with obesity is generated by spatiotemporal differences in macrophage subtypes. *Diabetes* **2008**, *57*, 3239–3246. [CrossRef]
105. Russo, L.; Lumeng, C.N. Properties and functions of adipose tissue macrophages in obesity. *Immunology* **2018**, *155*, 407–417. [CrossRef] [PubMed]
106. Bourlier, V.; Zakaroff-Girard, A.; Miranville, A.; De Barros, S.; Maumus, M.; Sengenes, C.; Galitzky, J.; Lafontan, M.; Karpe, F.; Frayn, K.N.; et al. Remodeling phenotype of human subcutaneous adipose tissue macrophages. *Circulation* **2008**, *117*, 806–815. [CrossRef] [PubMed]
107. Chylikova, J.; Dvorackova, J.; Tauber, Z.; Kamarad, V. M1/M2 macrophage polarization in human obese adipose tissue. *Biomed. Pap. Med. Fac. Univ. Palacky Olomouc Czechoslov.* **2018**, *162*, 79–82. [CrossRef]
108. Strand, K.; Stiglund, N.; Haugstøyl, M.E.; Kamyab, Z.; Langhelle, V.; Lawrence-Archer, L.; Busch, C.; Cornillet, M.; Hjellestad, I.D.; Nielsen, H.J.; et al. Subtype-Specific Surface Proteins on Adipose Tissue Macrophages and Their Association to Obesity-Induced Insulin Resistance. *Front. Endocrinol.* **2022**, *13*, 856530. [CrossRef] [PubMed]
109. Finlin, B.; Memetimin, H.; Confides, A.; Zhu, B.; Westgate, P.; Dupont-Versteegden, E.; Kern, P. Macrophages expressing uncoupling protein 1 increase in adipose tissue in response to cold in humans. *Sci. Rep.* **2021**, *11*, 23598. [CrossRef] [PubMed]
110. Tanaka, M.; Ikeda, K.; Suganami, T.; Komiya, C.; Ochi, K.; Shirakawa, I.; Hamaguchi, M.; Nishimura, S.; Manabe, I.; Matsuda, T.; et al. Macrophage-inducible C-type lectin underlies obesity-induced adipose tissue fibrosis. *Nat. Commun.* **2014**, *5*, 4982. [CrossRef]
111. Gericke, M.; Weyer, U.; Braune, J.; Bechmann, I.; Eilers, J. A method for long-term live imaging of tissue macrophages in adipose tissue explants. American journal of physiology. *Endocrinol. Metab.* **2015**, *308*, E1023–E1033.
112. Cinti, S.; Mitchell, G.; Barbatelli, G.; Murano, I.; Ceresi, E.; Faloia, E.; Wang, S.; Fortier, M.; Greenberg, A.S.; Obin, M.S. Adipocyte death defines macrophage localization and function in adipose tissue of obese mice and humans. *J. Lipid Res.* **2005**, *46*, 2347–2355. [CrossRef]
113. Nawaz, A.; Tobe, K. M2-like macrophages serve as a niche for adipocyte progenitors in adipose tissue. *J. Diabetes Investig.* **2019**, *10*, 1394–1400. [CrossRef]
114. Gaens, K.H.; Stehouwer, C.D.; Schalkwijk, C.G. Advanced glycation endproducts and its receptor for advanced glycation endproducts in obesity. *Curr. Opin. Lipidol.* **2013**, *24*, 4–11. [CrossRef] [PubMed]
115. Ruiz, H.H.; Ramasamy, R.; Schmidt, A.M. Advanced Glycation End Products: Building on the Concept of the "Common Soil" in Metabolic Disease. *Endocrinology* **2020**, *161*, bqz006. [CrossRef] [PubMed]
116. Wang, Z.; Wang, D.; Wang, Y. Cigarette Smoking and Adipose Tissue: The Emerging Role in Progression of Atherosclerosis. *Mediat. Inflamm.* **2017**, *2017*, 3102737. [CrossRef] [PubMed]
117. Solberg, L.I.; Desai, J.R.; O'Connor, P.J.; Bishop, D.B.; Devlin, H.M. Diabetic patients who smoke: Are they different? *Ann. Fam. Med.* **2004**, *2*, 26–32. [CrossRef] [PubMed]
118. Cai, X.; Chen, Y.; Yang, W.; Gao, X.; Han, X.; Ji, L. The association of smoking and risk of diabetic retinopathy in patients with type 1 and type 2 diabetes: A meta-analysis. *Endocrine* **2018**, *62*, 299–306. [CrossRef] [PubMed]
119. Sari, M.I.; Sari, N.; Darlan, D.M.; Prasetya, R.J. Cigarette Smoking and Hyperglycaemia in Diabetic Patients. *Open Access Maced. J. Med. Sci.* **2018**, *6*, 634–637. [CrossRef] [PubMed]

120. Choi, S.K.; Kim, C.K.; Jo, D.I.; Lee, M.C.; Kim, J.N.; Choi, H.G.; Shin, D.H.; Kim, S.H. Factors Associated with a Prolonged Length of Hospital Stay in Patients with Diabetic Foot: A Single-Center Retrospective Study. *Arch. Plast. Surg.* **2017**, *44*, 539–544. [CrossRef] [PubMed]
121. Hansson, B.; Moren, B.; Fryklund, C.; Vliex, L.; Wasserstrom, S.; Albinsson, S.; Berger, K.; Stenkula, K.G. Adipose cell size changes are associated with a drastic actin remodeling. *Sci. Rep.* **2019**, *9*, 12941. [CrossRef] [PubMed]
122. Kim, K.K.; Sheppard, D.; Chapman, H.A. TGF-β1 Signaling and Tissue Fibrosis. *Cold Spring Harbor Perspect. Biol.* **2018**, *10*, a022293. [CrossRef]
123. Sun, K.; Tordjman, J.; Clement, K.; Scherer, P.E. Fibrosis and adipose tissue dysfunction. *Cell Metab.* **2013**, *18*, 470–477. [CrossRef]
124. Francis, M.P.; Sachs, P.C.; Madurantakam, P.A.; Sell, S.A.; Elmore, L.W.; Bowlin, G.L.; Holt, S.E. Electrospinning adipose tissue-derived extracellular matrix for adipose stem cell culture. *J. Biomed. Mater. Res. Part A* **2012**, *100*, 1716–1724. [CrossRef] [PubMed]
125. Di Caprio, N.; Bellas, E. Collagen Stiffness and Architecture Regulate Fibrotic Gene Expression in Engineered Adipose Tissue. *Adv. Biosyst.* **2020**, *4*, e1900286. [CrossRef] [PubMed]
126. Ricard-Blum, S. The collagen family. *Cold Spring Harbor Perspect. Biol.* **2011**, *3*, a004978. [CrossRef] [PubMed]
127. Karsdal, M.A.; Nielsen, S.H.; Leeming, D.J.; Langholm, L.L.; Nielsen, M.J.; Manon- Jensen, T.; Siebuhr, A.; Gudmann, N.S.; Ronnow, S.; Sand, J.M.; et al. The good and the bad collagens of fibrosis-Their role in signaling and organ function. *Adv. Drug Deliv. Rev.* **2017**, *121*, 43–56. [CrossRef]
128. Johannsen, D.L.; Tchoukalova, Y.; Tam, C.S.; Covington, J.D.; Xie, W.; Schwarz, J.-M.; Bajpeyi, S.; Ravussin, E. Effect of 8 Weeks of Overfeeding on Ectopic Fat Deposition and Insulin Sensitivity: Testing the "Adipose Tissue Expandability" Hypothesis. *Diabetes Care* **2014**, *37*, 2789–2797. [CrossRef] [PubMed]
129. Strieder-Barboza, C.; Baker, N.A.; Flesher, C.G.; Karmakar, M.; Neeley, C.K.; Polsinelli, D.; Dimick, J.B.; Finks, J.F.; Ghaferi, A.A.; Varban, O.A.; et al. Advanced glycation end-products regulate extracellular matrix-adipocyte metabolic crosstalk in diabetes. *Scientific Reports* **2019**, *9*, 19748. [CrossRef] [PubMed]
130. Maeda, N.; Shimomura, I.; Kishida, K.; Nishizawa, H.; Matsuda, M.; Nagaretani, H.; Furuyama, N.; Kondo, H.; Takahashi, M.; Arita, Y.; et al. Diet-induced insulin resistance in mice lacking adiponectin/ACRP30. *Nat. Med.* **2002**, *8*, 731–737. [CrossRef] [PubMed]
131. Zeyda, M.; Huber, J.; Prager, G.; Stulnig, T.M. Inflammation correlates with markers of T-cell subsets including regulatory T cells in adipose tissue from obese patients. *Obesity* **2011**, *19*, 743–748. [CrossRef] [PubMed]
132. Buechler, C.; Krautbauer, S.; Eisinger, K. Adipose tissue fibrosis. *World J. Diabetes* **2015**, *6*, 548–553. [CrossRef]
133. Beltowski, J. Adiponectin and resistin—New hormones of white adipose tissue. *Med. Sci. Monit.* **2003**, *9*, RA55–RA61.
134. Kern, P.A.; Di Gregorio, G.B.; Lu, T.; Rassouli, N.; Ranganathan, G. Adiponectin Expression from Human Adipose Tissue. *Diabetes* **2003**, *52*, 1779–1785. [CrossRef] [PubMed]
135. Wang, J.; Leclercq, I.; Brymora, J.M.; Xu, N.; Ramezani-Moghadam, M.; London, R.M.; Brigstock, D.; George, J. Kupffer cells mediate leptin-induced liver fibrosis. *Gastroenterology* **2009**, *137*, 713–723. [CrossRef] [PubMed]

Disclaimer/Publisher's Note: The statements, opinions and data contained in all publications are solely those of the individual author(s) and contributor(s) and not of MDPI and/or the editor(s). MDPI and/or the editor(s) disclaim responsibility for any injury to people or property resulting from any ideas, methods, instructions or products referred to in the content.